T.C.
ISTANBUL AYDIN UNIVERSITY
INSTITUTE OF GRADUATE STUDIES

A NOVEL MODIFIED CONTROL METHOD IN GRIDTIED PHOTOVOLTAIC SYSTEM

MASTER'S THESIS

Mousa MOHAMMED

Department of Electrical & Electronic Engineering
Electrical and Electronics Engineering Program

February , 2022

T.C.
ISTANBUL AYDIN UNIVERSITY
INSTITUTE OF GRADUATE STUDIES

A NOVEL MODIFIED CONTROL METHOD IN GRIDTIED PHOTOVOLTAIC SYSTEM

MASTER'S THESIS

Mousa MOHAMMED
(Y2013.300005)

Department of Electrical & Electronic Engineering
Electrical and Electronics Engineering Program

Thesis Advisor: Prof. Dr. Murtaza FARSADI

February , 2022

APPROVAL PAGE

DECLARATION

I hereby declare with respect that the study “A Modified Control Scheme in Grid-Tied Photovoltaic System”, which I submitted as a Master thesis, is written without any assistance in violation of scientific ethics and traditions in all the processes from the Project phase to the conclusion of the thesis and that the works I have benefited are from those shown in the Bibliography. (20/02/2022)

Mousa MOHAMMED

FOREWORD

I would like to thank my supervisior for his endless passion, And also i would like to thank the institute of applied science of Istanbul Aydin University, Department of Electrical and Electronic Engineering, all of my friends and every person who gave me any support or advice which help me in my work.

February, 2022 **Mousa MOHAMMED**

TABLE OF CONTENT

Page

ABBREVIATIONS

AC	**:** Alternating Current
DC	**:** Direct Curent
PWM	**:** Pulse With Modulation
SPWM	**:** Sinusoidal Pulse With Modulation
MROGI	**:** Modified Reduced Order Generalized Integrator
MPPT	**:** Maximum Power Point Tracker
PV	**:** Photo Voltaic Panel
APF	**:** Active Power Filters
PF	**:** Passive Filters
SRF	**:** Synchronous Reference Frame
ADALINE	**:** Adaptive Linear Element
CBF	**:** Complex Band-pass Filter
FO	**:** First Order
FC	**:** Fundamental Contituent
FF	**:** Fundamental Frequency
ILF	**:** In-loop Filter
CC	**:** Continuous Conduction
ICN	**:** Incremental Conductance
P&O	**:** Pertube and Observe
FPID	**:** Fuzzy Tuned PID

LIST OF FIGURES

Page

LIST OF TABLES

Page

A NOVEL MODIFIED CONTROL METHOD IN GRIDTIED PHOTOVOLTAIC SYSTEM

ABSTRACT

In this thesis, a new method for modified reduced order generalized integrator-based frequency locked loop (MROGI-FLL), for controlling the interfacing inverter of the grid-tied PV system to mitigate the harmonics. To minimize the steady-state error we used a Fuzzy tuned PID (FPID). The comparative study and methods of the proposed scheme are compared with existing and adaptive control techniques by using Matlab/Simulink, this new circuit topology, voltage level can be maintained and constant at the common DC-bus terminals, by using combining of some active components which are PWM and PV array, and Control methods, and external loads. Therefore, it can control the DC-DC converter which maximizes the power yield from the PV system. The presented MROGI_FLL control strategy appropriately compensates the load and grid harmonics, by adaptively assessing the amplitude, frequency, and phase angle.

Key Words: *Grid, PWM, PV, Photovoltaic, Filter, Active power, power quality, PV system, ROGI, MROGI, FLL FPID, APF, inductor, capacitor, MOSFET, Control system*

GÜÇ KALİTESİNİ ARTIRMA İÇİN ŞEBEKE BAĞLI FOTOVOLTAİK SİSTEMDE YENİ BİR MODİFİYE KONTROL ŞEMASI

ÖZET

Bu tezde, harmonikleri azaltmak için şebekeye bağlı PV sisteminin arabirim inverterini kontrol etmek için değiştirilmiş azaltılmış sıralı genelleştirilmiş entegratör tabanlı frekans kilitli döngü (MROGI-FLL) için yeni bir yöntem. Kararlı durum hatasını en aza indirmek için bir Bulanık ayarlı PID (FPID) kullandık. Önerilen şemanın karşılaştırmalı çalışması ve yöntemleri, Matlab/Simulink kullanılarak mevcut ve uyarlamalı kontrol teknikleri ile karşılaştırılmıştır, bu yeni devre topolojisi, bazı aktif bileşenlerin birleştirilmesiyle ortak DC-bus terminallerinde voltaj seviyesi ve sabit tutulabilir. bunlar PWM ve PV dizisi ve Kontrol yöntemleri ve harici yüklerdir. Bu nedenle, PV sisteminden güç verimini maksimize eden DC-DC dönüştürücüyü kontrol edebilir. Sunulan MROGI_FLL kontrol stratejisi, genliği, frekansı ve faz açısını uyarlamalı bir şekilde değerlendirerek yük ve şebeke harmoniklerini uygun şekilde telafi eder.

Anahtar Kelimeler: *Şebeke, PWM, PV, Fotovoltaik, Filtre, Aktif güç, güç kalitesi, PV sistemi, ROGI, MROGI, FLL FPID, APF, indüktör, kapasitör, MOSFET, Kontrol sistemi*

I. INTRODUCTION

A. Overview

The nonlinear switching properties of power electronic equipment in renewable energy systems result in current and voltage harmonics, which degrade the quality of the power delivered by these systems. As a result, electronics linked to the grid have a shorter lifespan due to harmonic interference. Because of this, research into power factor correction and harmonic reduction is a major focus of the field. [1]

Passive Filters (PF) have long been used to minimize harmonics, but they have a number of drawbacks, including their vast size, resonance issues, and set filter properties. To overcome the above disadvantages, active power filters (APFs) have been introduced [2], [3]. Current and voltage harmonics are better eliminated by APFs. Shunt APFs and series APFs are the two basic varieties. Current harmonics are removed using shunt APFs, whereas voltage harmonics are removed using series APFs.

B. Problem Statement

The topic of this thesis has massive area to be done from all sides, because there are various adaptive control approaches have been explored in recent years, such as recursive least squares (RLS) [13], least mean squares (LMS) [14], least mean fourth (LMF) [15], improved linear sinusoidal tracer (ILST) [16], variable step size least mean squares (VSSLMS) [17], and adaptive notch filter (ANF) [18]. However, they have some drawbacks, e.g., in terms of tracking the steady-state response, due to the 4th-order optimization, high complexity, high computational cost, and poor convergence rate, this is not a suitable solution.

C. Objectives of the Study

Adaptive modified ROGI-FLL control system is utilized to extract the FC from load currents and grid voltages, resulting in anti-harmonic current generation using a PWM controller, which is the primary objective of this work. MATLAB/SIMULINK and Algorithms are the tools that we rely on.The main goals of the study are given below:

- To see which control methods is more efficiency and better in real-life.
- Maintaining a constant voltage at the common dc-link terminals is important for reducing steady-state error.
- A comparison of the proposed method of control with many other methods of control.

D. Description of Project

This thesis focuses on modifying the traditional ROGI-based FLL (ROGI-FLL) using a suggested topology, which we shall study in detail in chapter 3. As a result, this is the primary goal of our thesis.

E. Methods

Grid-tied photovoltaic (PV) systems may minimize harmonics by using modified control mechanisms in grid-tied systems. Making a realistic test of the suggested topology is made possible with the usage of MATLAB/Simulink software. Our suggested high gain DC-DC converter architecture, which utilizes power electronic switches, inductor, capacitor, and a PV array, was simulated using MPPT algorithms and a PV array as the DC input to the simulation program.

F. Outline of a Dissertation

The following are the chapters that make up the framework of the thesis:

Chapter I, This chapter serves as an introduction.

Chapter II, An overview of the research on power converter

topologies, including studies on their properties and comparisons, is presented in this chapter.

Chapter III In this chapter, the thesis approach, simulation, and circuit are briefly discussed.

Chapter IV, This chapter contains the results and discussion of four case studies that were compared to one another.

II. REVIEW OF STUDIES

A. Preface

The theoretical underpinning of Photovoltaic (PV) systems is discussed in this portion of the thesis.

An inverter and various electrical and mechanical equipment are used to convert the sun's rays into power in a photovoltaic (PV) system.

Off-grid PV systems are also possible with PV systems. As the name suggests, "photovoltaic" is made up of two words: Photo and Volt.

One of the most important sources of renewable energy is the electrical phenomena system of the stars. There are several benefits to using solar power, including the fact that it doesn't pollute, has no upkeep, and can be used again and over again. The basic device of an electrical phenomenon system is the cell. Cells are also classified to create panels or modules. Panels are classified to create massive electrical phenomenon arrays. The term array is sometimes utilized to explain an electrical phenomenon panel (with many cells connected nonparallel and/or parallel) or a bunch of panels. However, There is still a lot of improvement in the PV system's efficiency. In fact, the PV module's capacity to generate power relies on a variety of factors, including irradiance, temperature, and the current drawn from the battery. At the MPP (Maximum Power Point), the PV operates at its highest potency Therefore, to extract the utmost power underneath the various conditions explicit earlier, the most outlet following (MPPT) technique is employed to regulate the unsteady operational outlet of the PV array via a DC-DC converter. [22]

Figure 2.1 depicts the photovoltaic phenomenon, in which sunlight, composed of energy packets called photons, strikes a solar array and generates an electrical current. Each solar panel generates a little amount of electricity, but they are commonly joined together to form a solar battery. [19]. There is a DC-DC kind of power generated by a solar array. As a result, in order to make use

of solar power, an inverter is required to convert it from DC to AC. When the inverter generates AC energy, it may be utilized to power local devices, or it can be routed to the grid to be used elsewhere. [19].

Figure 2.1: Works of the PV system

B. PV System Components

PV system has consisted a [Cell, Modul, Panel, String, Subarray, Array], A PV cell, conjointly unremarkably known as a photovoltaic cell, is that the elementary of a PV power grid. A crystalline-based photovoltaic cell options a contact. As shown within the figure 2.2. The producing method includes melting, doping, metallization, and texturing. The positive and negative sides of the junction kind the DC voltage of one contact cell is a smaller amount than one V, that is low for many sensible applications. Moreover, it's automatically fragile and should be laminated and guarded for sensible use. [19]

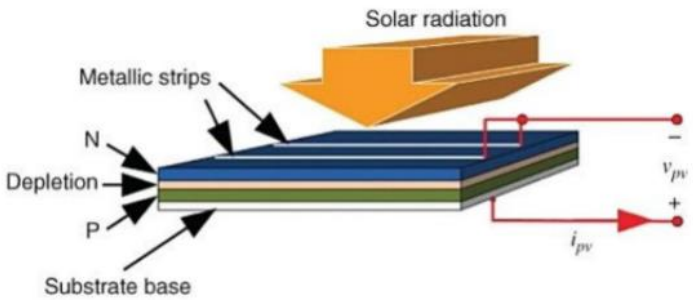

Figure 2.2: Construction of a crystalline photovoltaic cell.

The Photovoltaic system or solar panel, which can generate greater voltages and more power than a single cell, is the most important component for end consumers. The cells of a PV module are joined and laminated together. The number of cells in a PV module is no longer limited to the nominal voltages of battery or mass because of grid-connected installations and developments in power-conditioning equipment. There are two layers of substrate and superstrate sandwiching crystalline-based PV cells to create a PV panel. [19]

Tempered glass is frequently used as a superstrate, aiding module lamination and protecting sensitive cells. Because each area unit is made of semiconductor, glass has a quantitative relationship of thermal growth identical to that of a crystalline PV cell. Tempered glass is also strong and transparent, with around ninety-four light transmissions. In order to reduce light reflections, the glass surface is also not smooth. PV cells are connected in series using metal conductors that go from the surface to the bottom. The PV cells are protected by an encapsulant, which is a substance that sits between the superstrate and the substrate and surrounds the PV cells. [19]

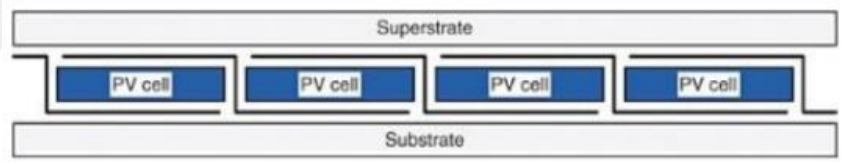

Figure 2.3: Lamination of PV module

During a series association, there are 72 cells in each. The cells are organized into three groups, each of which is called a submodule. There is a single bypass diode in each submodule, which is linked in parallel to 24 star cells. As illustrated in figure 2.4, the implementation eliminates the negative consequences of hot spots if the series-connected cells generate imbalanced power. [19]

There has to be more focus on the AC PV modules, or simply AC modules. Associate AC module is just a substitute for ordinary PV modules, consisting of linked star cells, a junction box, a superstrate, a substrate, electrical connectors, and different lamination parts, and is thus an environmentally protected item.

This is because the microinverter resolution, which converts DC to AC at the PV module level, is same.

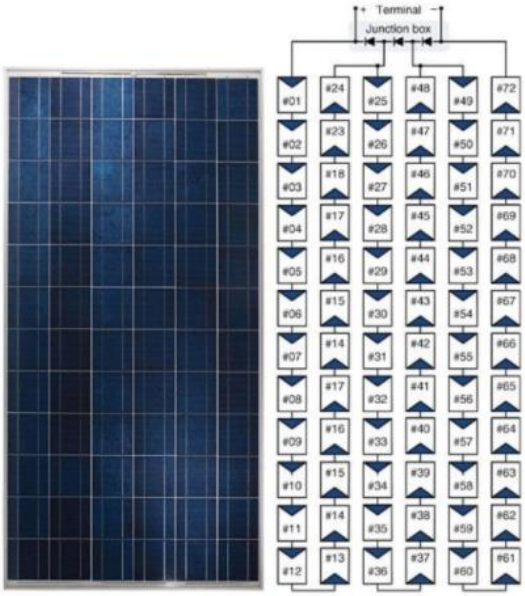

Figure 2.4: left, appearance; right, setup of a 72-cell PV module

To properly describe PV generators, it's critical to employ vocabulary like "cell," "module," "panel," "string," "subarray," and "array." Figure 2.5 shows how the ability capacity is built up from the cell level to the array level. Nonparallel and/or parallel configurations of PV modules are often used to build PV power systems. Stringing together star modules in order to increase output voltage is often referred to as "stringing." It is possible to create an array of PV strings that can generate hundreds, even millions, of watts by connecting them in parallel. Multiple subarrays are used in large-scale photovoltaic power plants. [19]

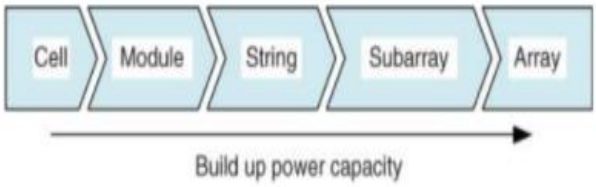

Figure 2.5: Components of PV system

Both monopolar and bipolar PV arrays may be found. There are two wires in the output circuit of a monopolar array or subarray, one positive (+) and the other negative (-). As seen in Figure 2.6, two monopolar subarrays form a bipolar PV array with a neutral function. Ideally, the power and voltage ratios of the twin monopolar subarrays should be forced to match. The neutral objective of the linked system is anchored in a core purpose. E energy is said to have been the

leading manufacturer of utility-interaction inverters for large-scale PV power systems and bipolar array configurations. The bipolar PV array's output is accommodated by the inverter, which has a maximum voltage rating of +600 V. [19]

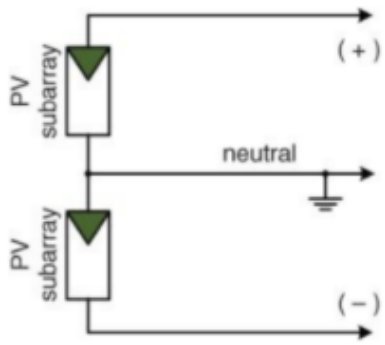

Figure 2.6: Bipolar PV array formed from two monopolar subarrays

C. PV Output Characteristics

It is customary to use the current-voltage (V) and power-voltage (PV) curves to depict the output results of PV cells and modules. These curves may also be used to depict the PV out place features in specific circumstances, such as in the case of a battery. Figure 2.7 depicts common I-V and P-V graphs for a PV cell's output, which may be applied to other devices. A PV module, string, or array may be represented by normalized curves after all of its star cells have been tested under identical circumstances. Figures represent the three critical points and four critical values that were listed in Table 2.1. To account for the nominal rating, some STC data is included in the data set. [19]

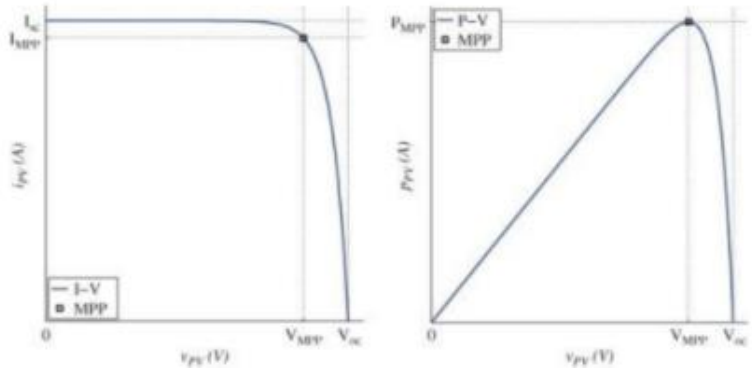

Figure 2.7: PV Output characteristics: I-V curves on the left and P-V curves on the right.

Table 2.1: Representative PV Output Characteristics include the following:

Symbol	Description
V_{OC}	When the PV output terminal is open-circuit and exhibiting zero current, the open-circuit voltage is monitored.
I_{SC}	When the PV generator terminal is short-circuited, the short-circuit current is measured.
I_{MPP}	At the MPP, the current is measured.
V_{MPP}	At the MPP, the voltage is measured.

It is computed as $P_{MPP} = V_{MPP} * I_{MPP}$ to determine the maximum power level for a given environment.

Variable depending on the surroundings. MPPT tracking is needed to determine the instantaneous maximum power point (MPP) dependent on the solar irradiation, cell temperature or other variables.

D. Standalone System

As far back as the 1950s, when PV technology was widely employed for home power supplies, stand-alone PV systems have been providing electricity to hundreds of people in rural areas. Radiation is more strong inside since the atmosphere and clouds do not attenuate or prevent it. When it comes to solar power production, the outside atmosphere is considered the ideal location. However, the majority of their recent use has been on Earth. Satellites, spaceships, housing stations, isolated residences, communities, street lamps, communication sites, pumping systems, and automobiles are all examples of independent systems. For large-scale solar energy production, the utility grid serves as an essential buffer to tolerate the intermittent nature of solar energy output. Grid-connected PV systems are now constructed in areas where grid connections are unachievable. DC, AC, or both may be provided by a standalone PV system depending on the need for power. Despite the lack of significant energy storage, PV producers may offer hundreds of kilowatts of electricity either directly or through power interfaces. Indirectly connected systems requiring voltage conversion may need the use of power conditioning instrumentality. The intermittent nature of PV power production necessitates energy storage in the majority of applications. For example, in Figure 2.8, a hybrid system may be powered by wind turbines, fuel cells or a traditional engine-based generator. [19]

Because the energy storage is a buffer, but not a source of electricity, a PV-battery system is not a hybrid system without additional resources. BOS encompasses everything between facility sources and the hundreds of components that make it up. To fill the battery bank, charge controllers are almost always required. BOS components like filters and protective devices are essential but not shown in Figure 2.8. [19]

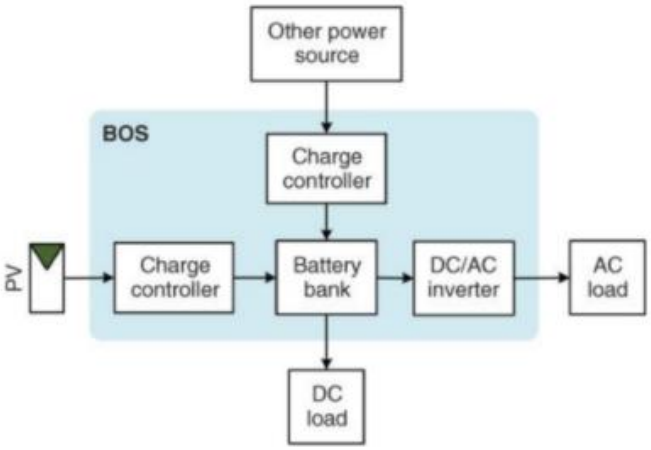

Figure 2.8: Power generation from photovoltaic panels and energy storage are included in this conventional system setup. BOS, or system balance.

E. DC Grid and Microgrid Connections

DC microgrids and DC distribution systems are gaining interest and have demonstrated the capacity to compete with traditional AC grids, even though a grid association is more crucial for AC grids.

HVDC systems have been put in place across the globe and have shown to be both effective and dependable for bulk and long-distance power transfer. Low-tension applications are another advantage of DC. All of the most popular electronic gadgets in the house are powered by DC power sources. These include phones and computers as well as printers and monitors. power consumption is significantly reduced in modern data centers thanks to standard and scalable DC power supplies. Induction and magnet synchronous motors have traditionally been powered by three-phase AC power. When it comes to variable-speed drives, DC has become a need because of the current developments in power physics and management engineering. The motor's performance is smooth, responsive, and cost-effective, all backed by DC power

sources. However, due to the current AC supply system, a two-stage conversion - from AC to DC to AC - is frequently required for many applications, resulting in significant losses. HVDC and LVDC have both been shown to be successful in industrial settings. For medium-voltage DC systems at the distribution level, their potential advantages over older medium-voltage AC systems are still under examination, albeit they are not as widely discussed as HVDC and LVDC systems. [19]

Figure 2.9 shows an example of an LVDC microgrid. Two DC distribution panels are shown linked by a conventional DC bus in the system. In order to support a wide range of power sources and loads, the system makes use of standardized DC buses. Since the DC voltage is the only variable that must be managed, connecting becomes simpler than in an AC system. For each electromagnetic unit, a power-conditioning circuit that is many and optimally managed is provided. PV generators' DC/DC power interfaces are often set to MPPT mode to make the most of the solar electricity they collect.

Balance between generation and freight is achieved by using battery storage devices. DC bus voltage is managed by regulating the charging and discharging of battery modules. PV power production is only permitted to be discontinued if it will overrun each load and also the battery in the MPP. An urban or suburban strategy may be used to facilitate the coordination of resources and freight. The droop approach is a common formula for decentralized administration and coordination among various sharing methods. There is also the option of using duplex DC/AC converters to link the AC grid. PV-powered DC microgrids may be configured as either an off-grid (separate) or AC grid-connected (separate) system, depending on the user's needs. [19].

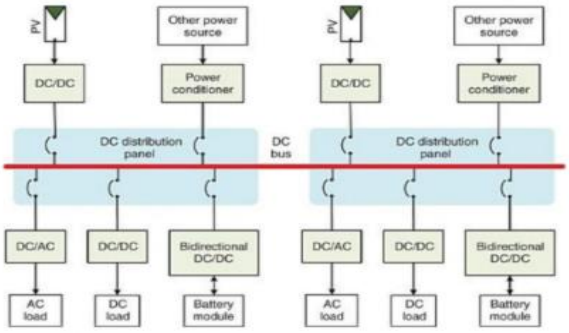

Figure 2.9: DC microgrid with PV power generation.

F. Maximum Power Point Tracking (MPPT)

Physicists Fuller and his colleagues were awarded a patent-pending prize in 1954 for their first sensible cell.

The output current (l) and voltage (V) of the PV module depend on the module's operational purpose whether it is currently connected to a resistive load, such as a DC lamp, as shown in Figure 2.10 or a dynamic load, such as a DC motor, as shown in Figure 2.11. Although the module l-V curve is non-linear with just one most electrical outlet (MPP) at the junction of the module and cargo -V curves, the module's operating function is located at the intersection of the module and cargo -V curves. As demonstrated in Figure 2.13, when the module/array is partially shaded, the P.V curve has several peaks as seen in Figure 2.14, indicating that the MPP has been relocated to a new place. [20]

Researchers have been pursuing the most electrical outlet chase (MPPT) since 1954 in an effort to raise PV system potency and improve performance.

A MPT may be classified into two types: mechanical single- and dual-axis trackers and electrical trackers. Using a "sun tracker," a mechanical huntsman, you may instruct the PV module to track the sun. However, this kind of implementation is expensive and time-consuming, and it has a poor potency. As a result, scientists' efforts are focused only on the pursuit of electricity.

The three groups of electrical MPPT approaches are as follows: Techniques used off-line, such as aliquot open-circuit (FOCV) and aliquot short-circuit (ASC).

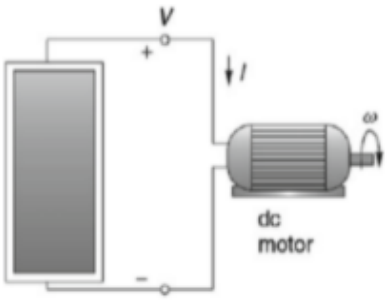

Figure 2.10: PV panel connected to a dynamic load

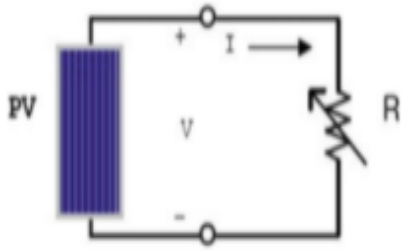

Figure 2.11: PV panel connected to a resistive load (R)

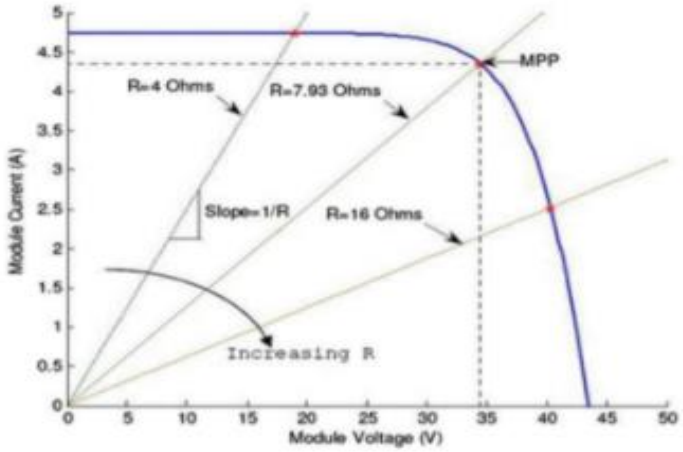

Figure 2.12: Location of operating point as influnced by load resistance (R)

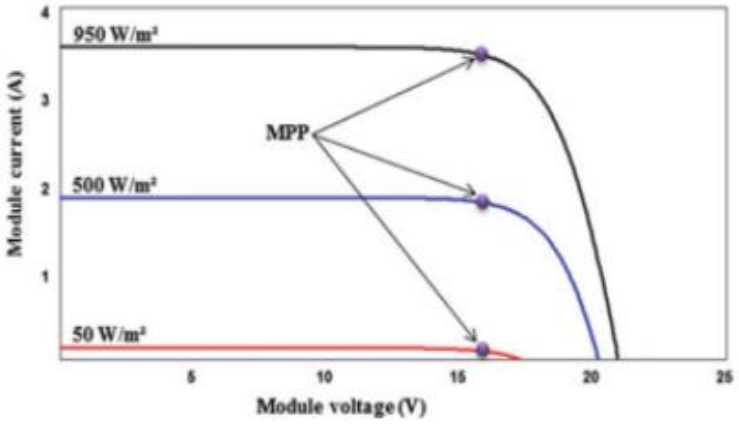

Figure 2.13: Location of MPP as influenced by irradiation level

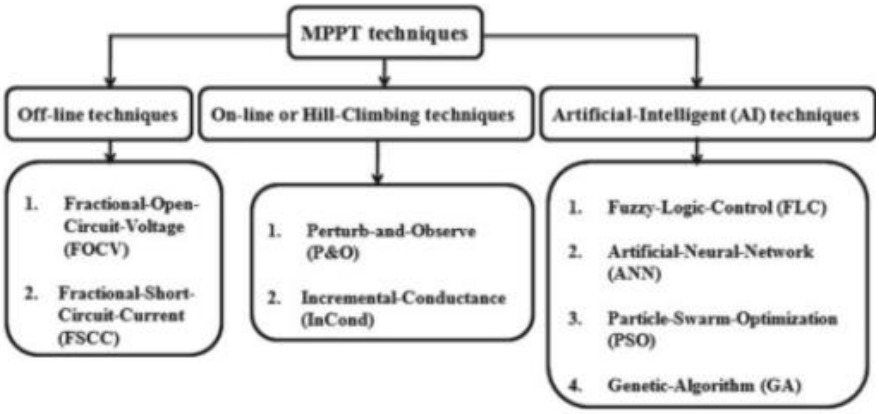

Figure 2.14: MPPT techniques

From 1954 to 2018, several methods and advancements have been documented in the scientific literature. Up until 1988, every studies on MPPT made use of a module or load to guarantee that the module and cargo current-voltage characteristic curves were as close to the MPP as possible. Many studies in this time attempted to identify the proper battery parameters to connect to the PV system in order to enhance the fit between module and cargo characteristics under varied irradiation levels and near temperatures. To show that the MPP is the intersection of the module's I-V curve and a resistive load's I-V curve, Hooke et al. performed style study in 1961. An experiment done in 1976 by Biran and colleagues confirmed that the MPP is the point where the I-V curves of a module and its dynamic load meet at the same location. For Braunstein's study in 1977, he found that the MPP is the point when /-V curves for both the module and battery load intersect. In 1977, Appelbaum narrowed his style analysis to resistive loads and storage. [20].

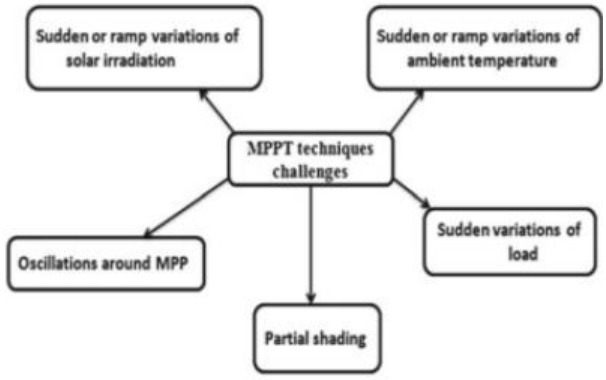

Figure 2.15: Challenges facing MPPT techniques

The MPPT controller are often accomplished supported completely different ways and algorithms. the foremost common ways area unit referred to as Perturb and Observe (P&O) and progressive electrical phenomenon (INC). This chapter treats the gathered modeling of a full electrical phenomenon system composed of an electrical phenomenon generator, power electronic parts, filter, and native masses. [22]

1. Modeling of the solar cell

Shockley's equation describes the electrical properties of a p-junction in a thin wafer or sheet of semiconductors, but the solar cell's p-junction is fictitious. As a result, a current source connected in series with a diode might serve as the most basic electrical cell equivalent circuit. Sunlight directly affects the amount of energy this source produces. A model of average quality was employed for this investigation. Figure 2.16 depicts the electric cell's circuitry.

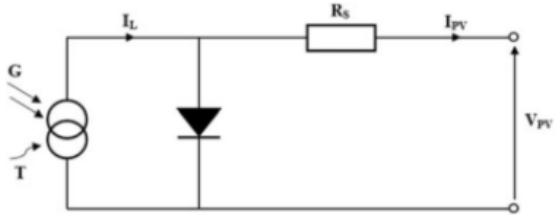

Fig. 1.1 Equivalent model of PV cell

Figure 2.16: Equivalent of PV cell

G. Photovoltaic Module

1. Effect of changes in parameters on the characteristics of PV module

At constant temperature (T = 25 °C), Figures 2.17 and 2.18 show the effects of varying irradiance (400 W/m2) on the PV's V_{pv} and P-V_{pv} characteristics. As can be seen, the module current and, therefore, the MPP, are directly proportional to irradiation, while the open-circuit voltage is only slightly affected. Figures 2.17 and 2.18.

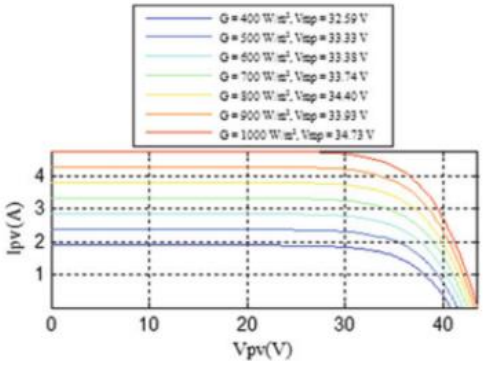

Figure 2.17: Effect of the irradiation on $I_{PV} - V_{PV}$ characteristic at T= 25 °C

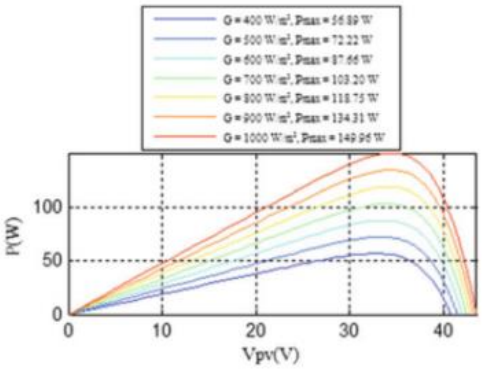

Figure 2.18: Effect of the irradiation on $P - V_{PV}$ characteristic at T= 25 °C

At constant irradiance (G = a 1000 W/m), the simulation results for different temperatures (T = 25°C, T = 50°C, T = 75°C) are given in Figures 2.19 and 2.20 for Ipv - Vpv and P - Vpv characteristics, respectively. On the basis of Figure 2.19, it can be seen that the produced power is gradually ablated, with the vast majority of it remaining available at low temperatures. Figure 2.20 shows that the current is constant up to a certain voltage, beyond which it gradually decreases. Once a PV module is connected directly to a load, its functioning is heavily reliant on the load's characteristics (see Figure 2.21). To put it another way, the load's electrical resistance governs the PV module's operating state, and only the best load, which goes through its characteristic MPP, can extract the greatest power. There is a strong likelihood that the MPP of the PV generator fluctuates constantly under changes in stellar irradiation and temperature.

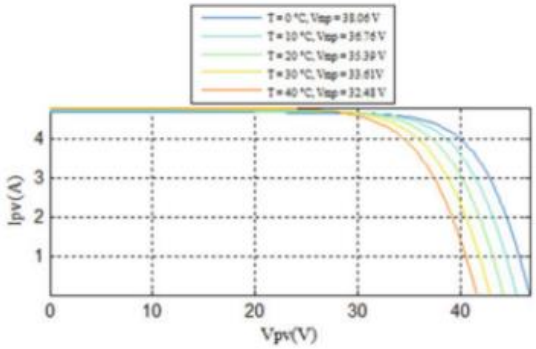

Figure 2.19: Effect of the temperature on $I_{PV} - V_{PV}$ characteristic at G=1000 W/m^2

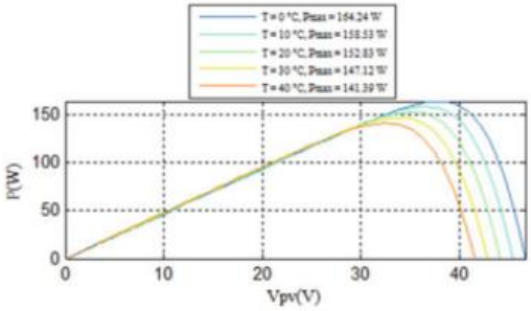

Figure 2.20: Effect of the temperature on $P - V_{PV}$ characteristic at G=1000 W/m^2

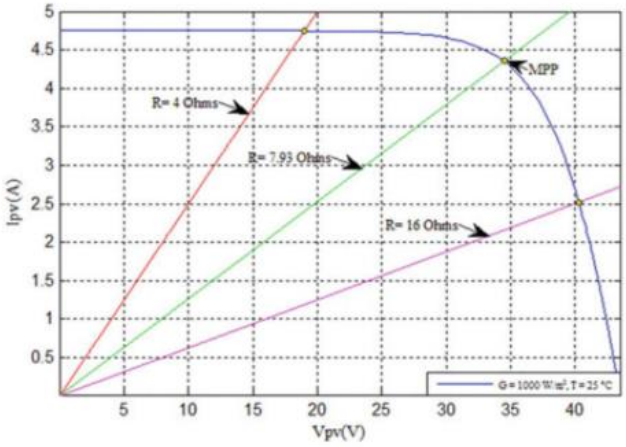

Figure 2.21: $I_{PV} - V_{PV}$ curves of PV module and various resistive loads simulated with the MATLAB model (G=1000 W/m2 , T = 25 °C).

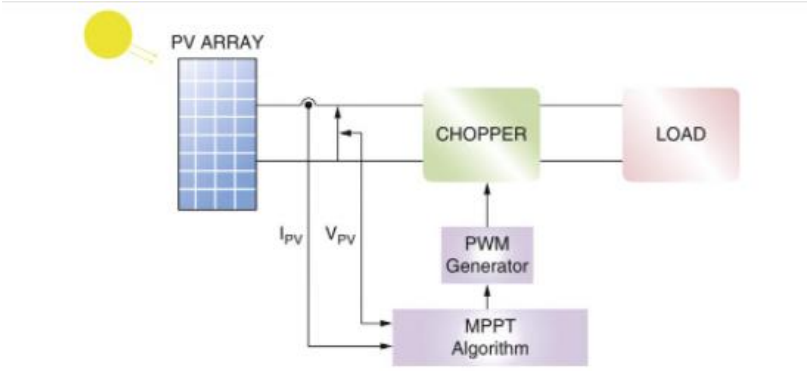

Figure 2.22: Block diagram of a PV array connected to the load

As well as electrical loads Thus, the MPPT approach is required to maximize the module's output and maximize the efficiency of PV cells.

2. MPPT techniques

MPPT is a self-adaptive system accustomed management a static device between the load and therefore the PV panel Figure 2.22. This device is intended to suit whenever the apparent resistivity of the load to the resistivity of the PV field appreciate the most outlet. This methodology relies on the utilization of a look formula of the most power of the electrical phenomenon panel curve. There are numerous different MPPT approaches in the literature, and the following sections outline the most often utilized ones. [22]

a. Perturbation and observation (P&O)

Because of its simplicity, the Perturb and Observe (P&O) algorithm is the most often used MPPT method. In Figure 2.23, if the PV array's operational voltage spikes in a certain direction and $\frac{dP}{dV} > 0$, A rumor has arisen that the array's operational intent toward the MPP was impacted by the disturbance. The P&O formula d p would then still perturb the PV array voltage within the same direction. If $\frac{dP}{dV} < 0$, In this case, the PV array was deleted from the MPP as a result of the change in operational purpose. As a result, the perturbation is reversed by using the P&O formula. Simple implementation is a benefit of the P&O approach. There are, however, certain restrictions. of steady-state functioning, such as oscillations around the MPP, sluggish reaction, and even lagging in the incorrect direction under rapidly dynamical area circumstances [22]

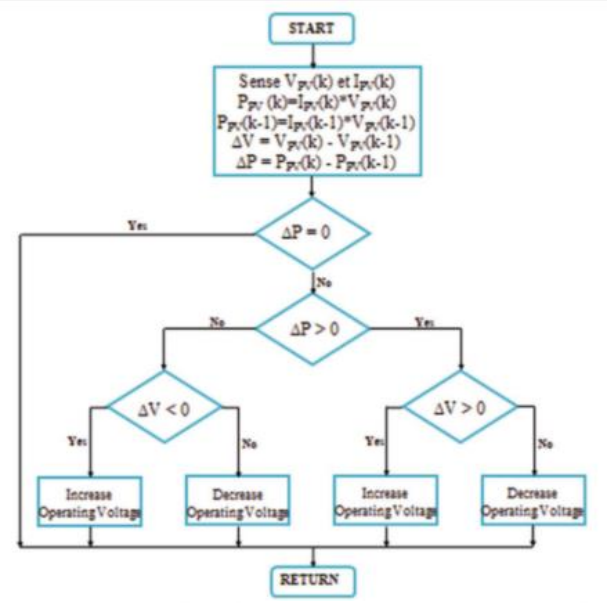

Figure 2.23: Flowchart of the P&O MPPT method

b. Incremental conductance (INC) method

The progressive electrical phenomenon uses the PV array's progressive electrical phenomenon $\frac{dP}{dV}$ to calculate the sign of dP/dV. This victimization is a phrase formed from the circumstance that exists at the MPP $\frac{dP}{dV}$ = zero. starting with this condition. it's doable to point out that, at the MPP $\frac{dI}{dV} + \frac{I}{V} = 0$. Thus, progressive electrical phenomenon will verify Also that MPPT has hit the MPP and is no longer disrupting the operation. Unless this need is fulfilled in its entirety, the direction in which the MPPT should be operating for its intended purpose will be estimated by using the relationship between $\frac{dI}{dV}$ and $-\frac{I}{V}$. The opposition will be able to monitor rapidly rising and falling irradiance conditions with more precision than P&O. Although this approach may produce oscillations around the MPP due to activity and division noise and error, it can also be confused in rapidly dynamic area settings due to these factors. In addition, the cumulative quality of this rule is worse than that of perturb and observe. Thus, the overall duration of the operation will be lengthened, and the array's voltage and current will be slowed down. It's shown in this figure. [22]

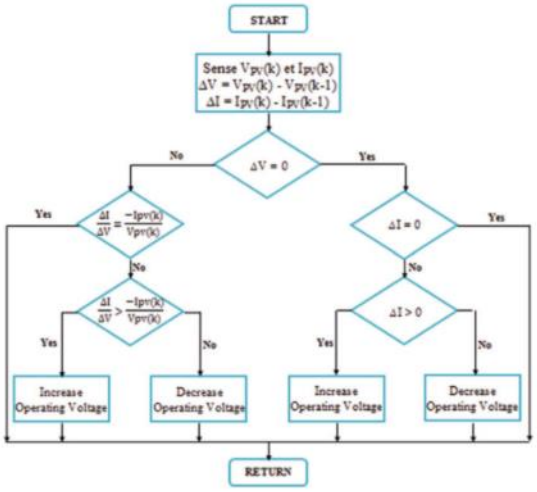

Figure 2.24: The INC MPPT method's flowchart

3. Simulation results

Figure 2.25 shows the PV system's modeling circuit in Matlab/Simulink. Two MPPT algorithms, P&O and INC, operate the Boost converter that connects the PV generator to a resistive load. As shown below, we varied the irradiation, temperature, and load to see how well the two methods (P&O and INC) performed under the identical simulated settings.

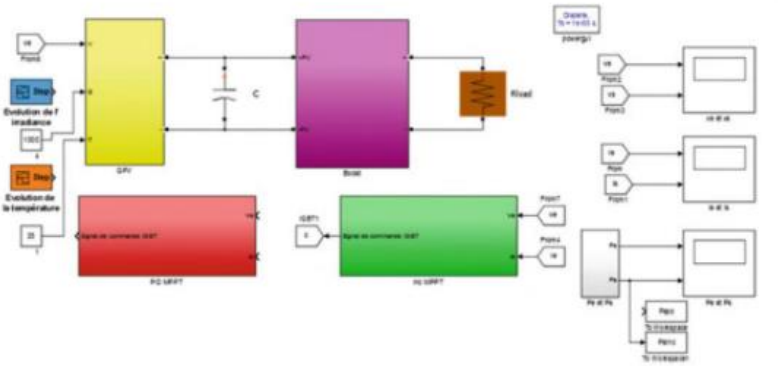

Figure 2.25: Matlab/Simulink environment for a photovoltaic system

a. Variation of irradiation

P&O and INC instructions are used in Figure 2.26 under various irradiation conditions to achieve convergence of PV system output power with MPP, as shown in Figure 2.27. [22]

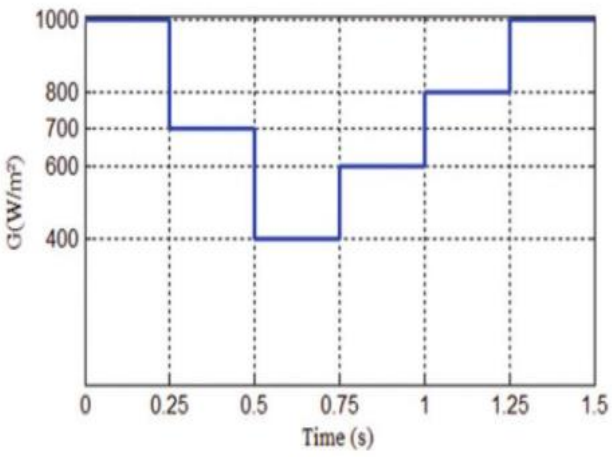

Figure 2.26: A PV system's output power over time as calculated by the P&O and INC algorithms at 25°C and various amounts of solar irradiation: 1000, 800, 700, 600, and 400 W/m^2.

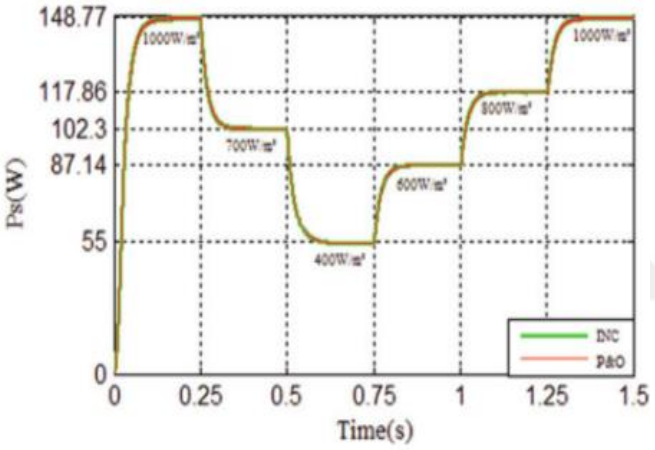

Fig. 1.15 Variation of solar irradiation

Figure 2.27: Variation of solar irradiation

b. Variation of temperature

Figure 2.28 shows how the PV system's output power converges to the MPP using P&O and INC instructions as seen in figure 2.28 as the temperature changes. [22]

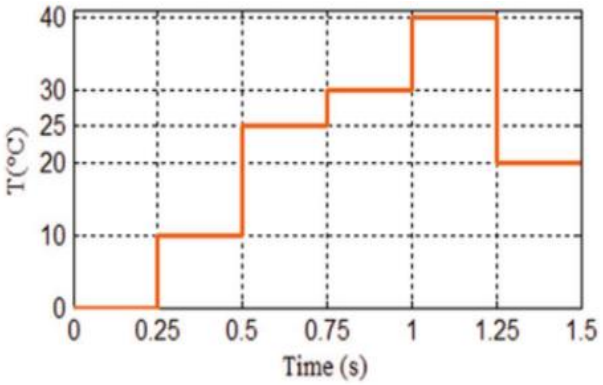

Fig. 1.16 Output power of the PV system verses time using P&O algorithm and INC algorithm at solar irradiation 1000 W/m^2 and different temperature levels 0, 10, 25, 30, 40 and 20 °C

Figure 2.28: Solar irradiation levels of 1000 W/m^2 and temperature levels of 0, 10, 25,30, 40, and 20°C were used to measure the output power from the Pv system over time.

4. DC voltage control

Figure 2.29 shows the PV system in its entirety. An MPPT algorithm might be used to manage the main DC/DC converter to ensure that the lower PV power can be raised to its maximum level under a variety of climatic conditions. In the second DC/DC converter, the input voltage may be raised to the level required by the VS, which operates with a harsh and rapid duty cycle, and the second DC/DC converter might be a boost. [22]

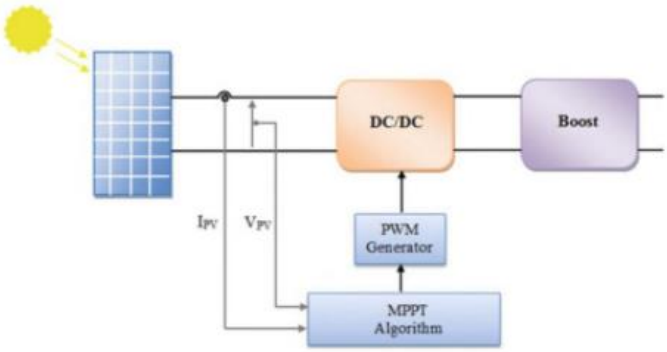

Figure 2.29: DC voltage control

5. PWM control

The VSI used here is a DC-to-AC three-phase converter. The electrical inverter's complicated circuit is shown in Figure 2.30. Three arms of the electrical inverter's facility are made up of one-two switches on each arm. A diode is connected in parallel to the semiconductors unit (IGBT, MOSFET...).

The pulse-width modulation (PWM) inverters produce high-order harmonics that are reduced by the L-C filter, which is coupled to the electrical converter output. [22]

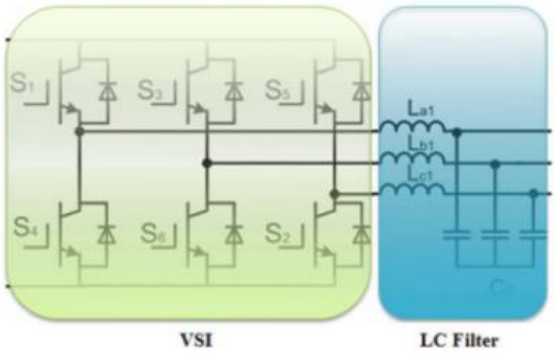

Figure 2.30: Three-phase VSI

Using a digital source to generate an analog signal is called pulse width modulation (PWM). PWM signals are defined by their duty cycle and frequency, which together determine their behavior. Using PWM, a fixed DC voltage may be converted to a variable DC voltage. THD (Total Harmonic Distortion) may be reduced by using PWM. Filtering a PWM inverter's output reduces distortion, which is an important consideration when trying to meet the THD specification. PWM modulation techniques include sinusoidal, hysteretic, space vector, and optimum, to name just a few of the most often used ones. The SPWM is utilized to regulate the inverter switching in this setup. As illustrated in Figure 2.31, the high-frequency triangular carrier wave VCR is compared to a sinusoidal frequency reference Vm in order to achieve SPWM and create the gating signal displayed in Figure 2.32 for the transistors. [22]

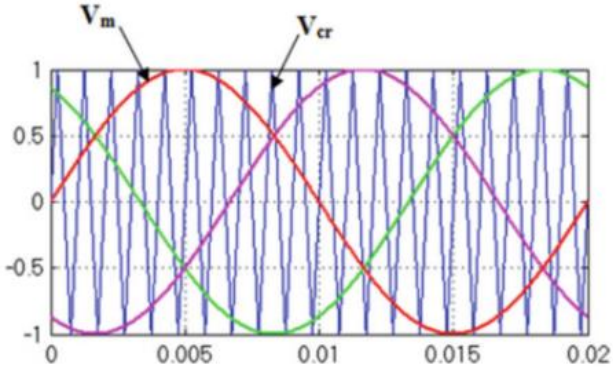

Figure 2.31: Reference voltage and triangle wave carrier

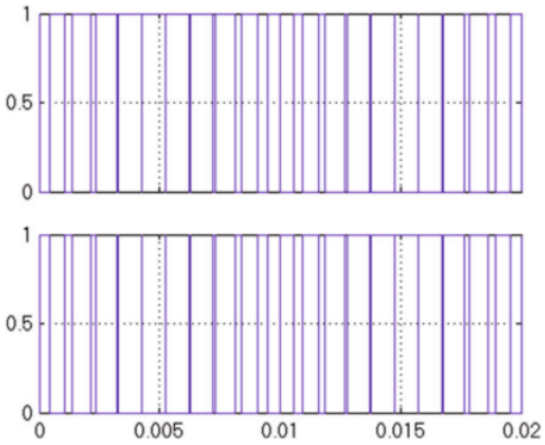

Figure 2.32: The inverter's first arm receives a pulse from the generator.

H. Types Of Photovoltaic And Battery Storage Systems

Arrays of photovoltaic modules (PV modules) are often used to increase the amount of electricity produced. The practical and operational requirements of star PV systems, as well as the element configurations, are often used to classify them. One might choose from a grid-connected, a PV hybrid or a whole star solar system. In the end, it all comes down to the patient's present energy supply, as well as what they want to get out of a certain system. Grid-connected and stand-alone systems are often categorized. [21]

1. PV system with a grid connection

PV systems that link to the grid To improve the electrical network's performance, it is common to put in measures to reduce facility losses and increase the voltage profile. These systems may have a lot of negative effects on a network if they are well-integrated [18], so this isn't always the case. It's possible to employ a grid-tied electrical converter and no battery storage in a grid-lied system. see Figure 2.33 for an example. This is an excellent option for those who want to add a star to their home but are already connected to the grid. These systems will be eligible for federal and state incentives that make it easier to get the system in the first place. Grid-tied systems are simple to design and very efficient due to the fact that they need a small number of components. The primary goal of a grid-tied system is to reduce your utility costs and enjoy the benefits of star incentives. Another problem is that when the facility goes down, so do all of your devices. Linemen working on the facility lines need to know

that there is no supply feeding the grid for safety reasons. Inverters that are connected to the grid must be forced to disengage mechanically when they lose contact with the grid. This means that you will be unable to provide electricity for the duration of an outage or emergency, and you will also be unable to store energy for later use. You may also be unable to control your system after you have used the service, such as during high demand times. It's not impossible to add battery storage later if you have a basic grid-tied system, but "the solution the associate degreaser" recommends is an AC-coupled system where the first grid-tied electrical converter is as well as a battery backup electrical converter. A excellent solution for those that need to put in a star now to take advantage of incentives, but can't afford to invest in the batteries, is this: A customer will enjoy web metering since they will be able to transmit electricity back to the grid when the star they are exploiting is no longer producing. the star will provide electricity to the masses at times when they are above what they are able to produce themselves. The star isn't the only source of power for the client. When the grid goes down, the star goes down as well as there is no battery backup in the system. [21]

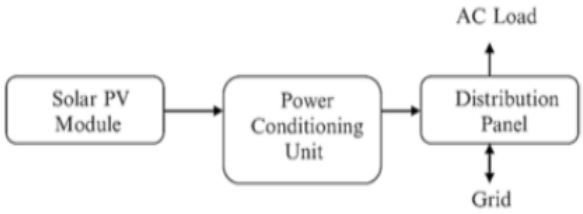

Figure 2.33: A schematic showing a grid-connected PV system's many components.

2. Powerful battery backup for grid-tied system

A grid-hybrid system, often known as a power network with battery backup, might be the next system type. Customers that are already connected to the grid and understand the need of having their own battery backup may benefit from this kind of system, as illustrated in Figure 2.34. This kind of system is ideal for consumers who are at risk of power outages in their region, or who just want to be prepared. [21]

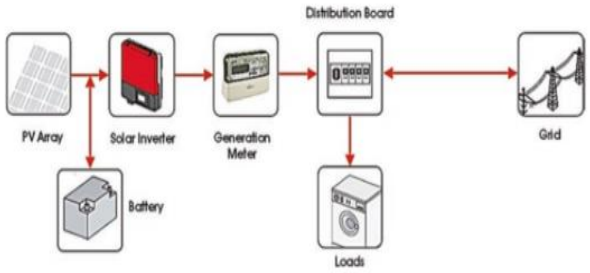

Fig. 1.4 Block diagram of grid-tied system with battery backup [19]

Figure 2.34: A schematic diagram of a battery-powered grid-tied system [21]

With this kind of system, you get the most effective of each world as a result of you are continuing to rely on the electricity grid may qualify for federal and state tax breaks while conjointly decreasing the cost of your power bill. At constant times, if there is a breakdown, you have got a backup. Associate in Nursing battery-based grid-tied systems provide power during an outage, and you'll be able to store energy for use in an emergency. You're able to keep a copy of essential masses like lighting and appliances once the facility is out. You'll also be able to consume energy during peak demand periods since you'll be storing it in your battery system for later use. The disadvantages of this strategy are that it places a higher importance on basic grid-tied systems and is less cost-effective. There are numerous components. The inclusion of the batteries necessitates the use of a battery bank to keep them safe. Should there even be a subpanel with all of the vital masses that need to be saved. The technology does not store all of the hundreds which the residence utilizes on the grid. A backup subpanel is used to isolate vital masses that are required when the grid power goes out.

I. Fuzzy

Using a broad definition, that is made of bulk of knowledge-based system (KBS) application to issues in closed-loop management, is also as follows: A KBS for the closed-loop system which reinforces the performance, responsibleness, and hardiness of management by incorporating information that that can't be accommodated within the analytic model upon that the planning of an effect algorithmic program relies, manual ways of operation, as well as other

safety and supporting logic procedures, are occasionally used to address this issue.

1. Fuzzy Control from an industrial perspective

Europe has caught the "fuzzy wave." Achievements in Japanese white goods and domestic physics have helped to boost the industry, well-liked however Furthermore, since 1990, there has been a tremendous increase in industry interest in fuzzy management, which was previously not considered as a serious field. However, there are still two dominating, extreme perspectives on the benefits of fuzzy management. The proponents of this technology argue, on the one hand, that it can change management engineering, promise huge advances, and be able to handle complex engineering difficulties with minimal effort However, some management engineers still believe that "anything that may be performed fuzzy administration is done traditionally as well" and that the "fuzzy buzz" will dissipate within the next several months. The realization that none of the two perspectives takes into consideration the significant potential of fuzzy management is barely bit by bit increasing, during this preface, we'll attempt to make a case for that, without a doubt, Various of the expectations sparked by popular news stories are overstated, although fuzzy management has significant advantages in several ways, which it is here to shine—in most situations as an undergrad degree add-on to conventional technology, and in other circumstances as an associate degree enabling technology: The most important reason it'll become an essential component of management engineering is also that fuzzy control may be a useful technology from an industrial standpoint. The objective of this article is to help you with your company, that is that the one we have a tendency to are taking here. In order to be ready to make a case for what the advantages of fuzzy management are, however, we have a tendency to initial can rethink it from 2 completely different technological views. [23]

2. Fuzzy Control's advantages

In light of present application of fuzzy management, that ranges from terribly tiny, home automation systems to large-scale process management systems rely on microcontrollers, the benefits of mistreatment fuzzy management square measure sometimes into one amongst the subsequent three classes.

a. Using expert knowledge to achieve a greater level of automation

The level of automation in industrial process control is often fairly low in the chemical sector. In order to start or stop a machine, to change the parameters of the controllers, or to move between various models of control, a human operator is required. This operator's knowledge is generally derived from personal experience and cannot be described in differential equations. A lot of the time, it's more of a "if I were in this circumstance, I'd do this instead" kind of scenario. The expert's knowledge may be represented and implemented via fuzzy control in this scenario. Let's take a look at the paper industry's digester management as an example. [23]

In conjunction to its process software, a Portuguese firm has installed a fuzzy-based digester control system. The essence of the operator's control approach is expressed using around twenty-five rules. The key advantage of achieving a greater degree of automation in this manner is the resultant constant control approach that can be implemented around the clock, resulting in a considerable decrease in quality of product variability (up to 60%). Furthermore, further software system improvements resulted in considerable energy and basic material usage reductions. Overall, after just a few months, the invest with in fuzzy control software suite and the level of knowledge of the real control system had paid for itself. [23]

b. Nonlinear control with a high degree of robustness

Consider the following scenario: Objects of varying masses must be moved along a route by a robotic arm with various linkages. Because reliable and realistic models of this system exist, implementing a PID controller that works pretty well for known masses within a restricted range should not be too difficult. [23]

Dramatic changes in parameters or large external disruptions, on the other hand, induce a significant decline in performance. In the face of such disturbances, PID systems must often choose between quick reactions with large overshoot and smooth but sluggish responses, or they may struggle to stabilize the system at all. In this scenario, fuzzy control allows for the implementation of simple but reliable solutions that span a broad range of system parameters and can even

withstand bigger disruptions. In this situation, a fuzzy sliding mode controller (see Chapter 4) was used, which performs similarly to the PID solution for a given mass with very modest variations, but outperforms it when greater fluctuations occur.

There are two additional advantages to employing fuzzy or hybrid solutions that have nothing to do with the control system's performance but are nonetheless essential from a commercial standpoint.[23]

c. Time to create and maintain is cut in half.

In certain circumstances, the construction of a control system involves two independent sets of specialists. Experts in the sector are familiar with the application issue and how to design effective control techniques. They are, however, often not electronics professionals who are familiar with numerical methods and microcontroller implementations. Electronics and system programmers who are unfamiliar with the application issue then carry out the real system implementation. This often results in communication issues between these two groups, causing delays and lengthier development timeframes. As previously stated, fuzzy control "lives" on two levels of abstraction and offers languages for both levels of expertise: the symbolic level is appropriate for articulating application engineers' techniques, while the compiled level is readily understood by electronics engineers. A fuzzy-based method may assist alleviate communication challenges since there is a well-defined formal translation between various levels. Consider idle control in automobile electronics, where complex control techniques must be designed and performed on basic 8-bit microcontrollers in time-critical scenarios. Aside from considerable variances in system characteristics owing to mass manufacturing and aging concerns, which need extensive system tuning, communication challenges between engine and microcontroller experts result in very extended development timeframes. We recently had the chance to evaluate two idle controllers, a traditional PID system, and a fuzzy control system on a test car. The control system's primary goal was to maintain an idle speed of 800 rpm independent of road conditions or extra energy users like power steering and air conditioning. There were almost no variations in the system's behavior, but the

fuzzy solution took just approximately six months to build, while the traditional approach took over two years to construct. [23]

J. The Calculations and Rules

We will show all rules and all calculation that we sued in this thesis.

1. Propsed control scheme

Mathematical analysis of the ROGI control scheme's modifications is as follows.

$$\frac{dI'_{l\alpha}}{dt} = -\omega' I'_{l\beta} + k(I_{l\alpha} - I'_{l\alpha}) - k'(I_{l\beta} - I'_{l\beta}) \quad \textbf{(1)}$$

$$\frac{dI'_{l\beta}}{dt} = -\omega' I'_{l\alpha} + k\left(I_{l\beta} - I'_{l\beta}\right) - k'(I_{l\alpha} - I'_{l\alpha}) \quad \textbf{(2)}$$

$$\frac{d\omega'}{dt} = \frac{\lambda}{I_1'^2}\left[I'_{l\alpha}\left(I_{l\beta} - I'_{l\beta}\right) - I'_{l\beta}(I_{l\alpha} - I'_{l\alpha}\right) = \frac{\lambda}{I_1'^2}\left[I'_{l\alpha} I_{l\beta} - I'_{l\beta} I_{l\alpha}\right] \quad \textbf{(3)}$$

$$\theta'_1 = \tan^{-1}\left(\frac{I'_{l\beta}}{I'_{l\alpha}}\right) \quad \textbf{(4)}$$

$$I'_1 = \sqrt{I'^2_{l\alpha} + I'^2_{l\beta}} \quad \textbf{(5)}$$

The estimated phase angle, estimated current amplitude, and estimated frequency are all included in this equation, as are the estimated error currents of the load current, the integral gain of the controller, the estimated phase angle, and the estimated amplitude and frequency of the load current, respectively. According to this formula, the cross-coupling gain term (kA') is determined. As an integral gain term, lambda (λ) is assumed to be 0.707 [24], which is large enough to ensure strong tracking performance while still maintaining the system's stability. Using LQR, the suggested control scheme's parameters may be fine-tuned [24]. Frequency, phase angle, amplitude tracking, and reference current computation are the four levels of the proposed control mechanism. Further subsections detail the mathematical analyses used to create the two steps.

a. Stage 1: tracking Frequency

(3) allows us to write as

$$\frac{d\omega'}{dt} = \frac{\lambda I_1 I_1'}{I'^2}[\cos(\theta_1')\sin(\theta_1) - \sin(\theta_1')\cos(\theta_1)] = \frac{\lambda I_1}{I_1'}[\sin(\theta_1 - \theta_1')] \quad \textbf{(6)}$$

Let us assume that $\theta_{1\approx}'\theta_1$ and $I_{1\approx}' I_1$, therefore (6) can be written as

$$\frac{d\omega'}{dt} \approx \lambda(\theta_1 - \theta_1') \quad \textbf{(7)}$$

$$\frac{d\Delta\omega'}{dt} \approx \lambda(\Delta\theta_1 - \Delta\theta_1') \quad \textbf{(8)}$$

Where $\Delta\omega'$ changes in the frequency of occurrence, $\Delta\theta_1'$and $\Delta\theta_1$ denotes the corresponding shift in phase angle.

b. Stage 2: current generation as a reference

The suggested algorithm's comprehensive control mechanism is provided in Chapter 3. The load current and line voltages must be extracted using FC, as well as the PV feedforward (pvff) and the unit vector template (UVT). The UVT is determined by monitoring grid voltages at the point of common connection, as shown below.

$$V_{t=}\sqrt{0.666(v_{pa}^2 + v_{pb}^2 + v_{pc}^2)} \quad \textbf{(9)}$$

Where $v_{pa}^2, v_{pb}^2, and v_{pc}^2$ are the grid voltages that are being sensed. The grid voltages' quadrature and in-phase UVT components are determined using (9).

$$v_{ia} = \frac{v_{pa}}{V_t}, v_{ib} = \frac{v_{pb}}{V_t}, v_{ic} = \frac{v_{pc}}{V_t} \quad \textbf{(10)}$$

Where via, vib, and vic are the line voltage in-phase components, and the UVT voltage is Vt. Hence, using (10), the line voltage quadrature UVT components are derived as follows.

$$v_{qa} = \frac{v_{ic}}{1.732} - \frac{v_{ib}}{1.732}, v_{qb} = \frac{1.732 * v_{ia}}{2} + \frac{(v_{ib} - v_{ic}) * v_{ib}}{3.464},$$

$$v_{qc} = -\frac{1.732 * v_{ia}}{2} + \frac{(v_{ib} - v_{ic}) * v_{ib}}{3.464} \quad \textbf{(11)}$$

A FC extracted the load currents are sampled and maintained in a ZCD unit using UVT quadrature components from the load currents. (v_{qa}, v_{qb}, and v_{qc}) to generate the currents' active power components (i_a, i_b, and i_c) generated by load.

The PV feedback control term, the active power components, and the current losing components of the DC controller are used to calculate the net part of the load currents, which is stated as follows.

$$i_{net} = \frac{i_a + i_b + i_c - I_{pvff}}{3} \quad \textbf{(12)}$$

Using the basic net component current, the computed reference currents are derived (I_{net}) also the in-phase UVT components via, v_{ib}, and v_{ic}, expressed as follows.

$$i_{ra} = i_{net} * i_{ia}, \quad i_{rb} = i_{net} * i_{ib}, \; i_{rc} = i_{net} * i_{ic} \quad \textbf{(13)}$$

The calculated reference currents (Ira, I_{rb}, and I_{rc}) and the actual grid currents (I_{sa}, I_{sb}, and I_{sc}) are sent into the PWM controller, which produces three-phase anti-harmonic currents that are injected into the power grid to reduce the harmonics and improve the power quality in the grid-integrated PV system.

2. DC Voltage normal FPID

Performance regulators based on P, PI, and PID models fail to stabilize the dc bus voltage during transients in the line and load. To overcome this deficiency, an adaptable PID management system with fuzzy tuning was developed to adaptively the transient conditions for calculating PID gains [25,26]. In Chapter 3, we see the FLPID's control diagram in action. The FLPID controller's mathematical modeling is described in detail below.

$$G_c(S) = k_p + \frac{k_i}{s} + k_p(s) \quad \textbf{(14)}$$

$$G_c(S) = k_p(1 + \frac{1}{\frac{k_p}{k_i}(s)} + \frac{k_d}{k_p}(s)) \quad \textbf{(15)}$$

Equation of the PID controller's discrete-time equivalent

$$u_k = k_p * e(k) + k_i . T_s \sum_{i=1}^{n} e(i) + \frac{k_d}{T_s} . e(k) - e(k-1) \quad \textbf{(16)}$$

In this case the error voltage, u_k e(k), is determined by subtracting the actual dc voltage from the reference dc voltage. In terms of mathematics, the following describes fuzzy gain scheduling for PID controllers:

$$k'_p = \frac{k_p - k_{p.min}}{k_{p.max} - k_{p.min}}, k'_d = \frac{k_d - k_{d.min}}{k_{d.max} - k_{d.min}} \quad \textbf{(17)}$$

Using the following formulae, the fuzzified results may be achieved.

$$k'_p = \sum_{i=1}^{m} \mu_i . k'_p . i \ , \ k'_d = \sum_{i=1}^{m} \mu_i . k'_d . i \ , \ \alpha = \sum_{i=1}^{m} \mu_i . k'_\alpha . i \quad \textbf{(18)}$$

Using the formulae below, the PID controller gains can be calculated

$$k_p = ((\big(k_{pmax} - k_{pmin}\big) . k'_p + k_{pmin}) \quad \textbf{(19)}$$

$$k_i = \frac{k_p^2}{\alpha . k_d} , k_d((k_{dmax} - k_{dmin}) . k'_d +$$

III. MATLAB/SIMULINK

A. Introduction

In this part, we'll quickly discuss the methods we use. Because it uses a PWM controller to create antiharmonic currents, the adaptive modified ROGI-FLL control scheme may be used to separate out the FC from load and grid voltages.

B. Proposed Topology Simulated Using Simulink

In this part, we will demonstrate a Simulink simulation of the suggested architecture, which includes power electrical parts and control elements, as well as a solar PV array, PWM, control system parts such as Capacitor, Resistance, Load, and Indictor. Maximum Power Point Tracking controller (MPPT), Three-phase voltage measurement, three phase source, Power measurement (Three-phase), and display, scope to monitor voltage and current and power the importance the system. In figure 3.1. existence of a generic simulation perspective In the sections that follow, we'll take a closer look at each individual simulation component.

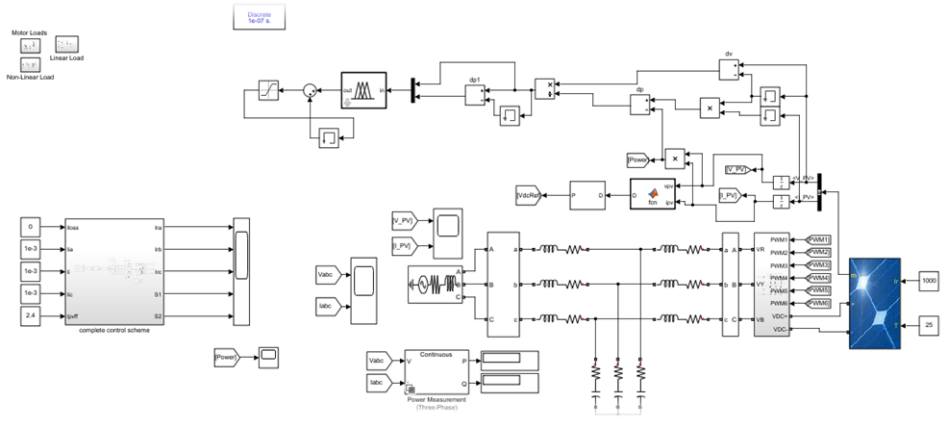

Figure 3.1: The whole simulation plan

For the purpose of this article, we will refer to the grid-tied electrical phenomena (PV) system power stage as Fig. 3.1. The system is made up of a two-stage PV system that feeds electricity into the grid. electrical phenomena

that is becoming better and better The maximum power point tracking (MPPT) approach is used, and a lift device is meticulously designed to take DC-bus capacitance design into account. Most likely, the boost device operates in CC mode with a high switching frequency. In this way, the size and cost of the inductance are minimized. If desired, the DC hundreds may be linked to the common DC-bus, which is common. Using the intended reference current generation approach, the FPID controller assures ripple-free DC-bus voltage and is coupled with the FC of the load current produced, resulting in reference currents for the APF electrical converter [25][26]. For the APF, a PMW controller creates the switch signals it needs. A filtering inductance is attached between both the APF and the AC bus in order to filter out high-order harmonics. The common AC bus connects a variety of linear and nonlinear hundreds to the electric grid. Work on a grid-tied system is coupled to a linear resistive-inductive load connected with an unregulated rectifier that operates as a nonlinear load.

1. PV Array

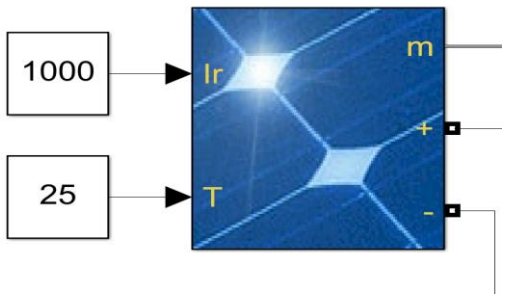

Figure 3.2: PV Array

Figure 3.3 shows a PV array for which we used a Soltech 1STH 215P P Panels Eleven parallel 3- series connection to achieve the desired voltage and power range.

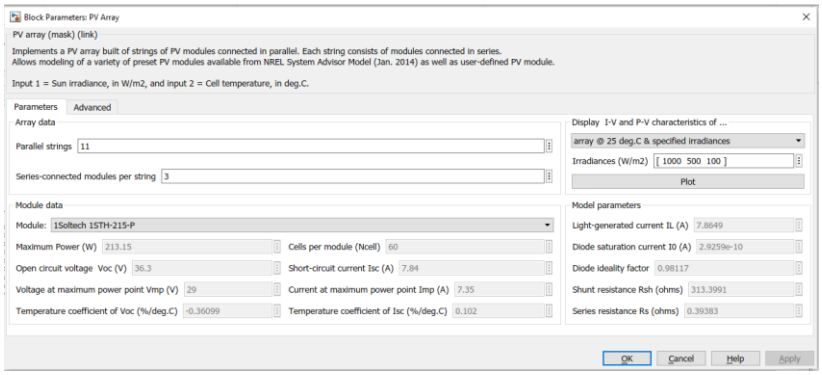

Figure 3.3: Array Specification for Presence PV

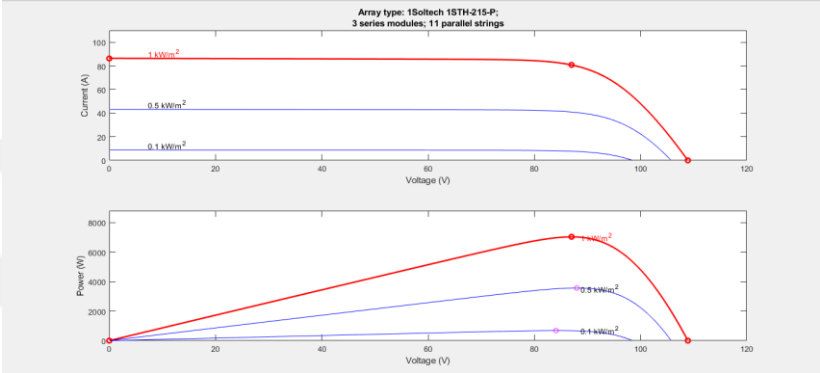

Figure 3.4: Voltage and current values at the highest points of a PV array

Figures 3.3 and 3.4 show the specifications of a presence PV array and the voltage, current, and power levels at their highest power points, respectively.

2. MPPT algorithm

The PV array voltage and current were measured using the P&O MPPT and IC MPPT algorithms. P&O MPPT algorithm code may be found here;

```
function D= fcn(vpv,ipv)

Dinit=0.4;

Dmax=0.9;

Dmin=0.1;

deltaD=20e-6;

persistent Vold Pold Dold;

dataType="double";

if isempty(Vold)
```

```
    Vold=0;
    Pold=0;
    Dold=Dinit;
end
P=vpv*ipv;
dV=vpv-Vold;
dP=P-Pold;
if dP~=0
    if dP<0
        if dV<0
            D=Dold-deltaD;
        else
            D=Dold+deltaD;
        end
    else
        if dV<0
            D=Dold+deltaD;
        else
            D=Dold-deltaD;
        end
    end
else  D=Dold;
 end
if D>=Dmax|D<=Dmin
    D=Dold;
end
```

Dold=D;

Vold=vpv;

Pold=P;

3. Icremental conductance (INC)

In this simulation, we employed both the P&O MPPT algorithm and INC MPPT to measure voltage and current readings from the PV array. We already showed P&O section, and now we can view the IC MPPT simulation below;

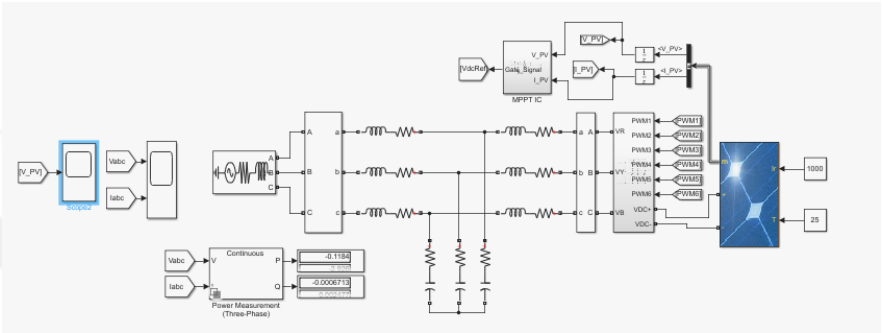

Figure 3.5: simulink of INC MPPT

4. PWM

We used PWM current controller to regulating the quantity of electricity given to a load while avoiding lost power. Additionally, use for filter out high order harmonics. We will presentin figure 3.6 the simulink of the PWM below;

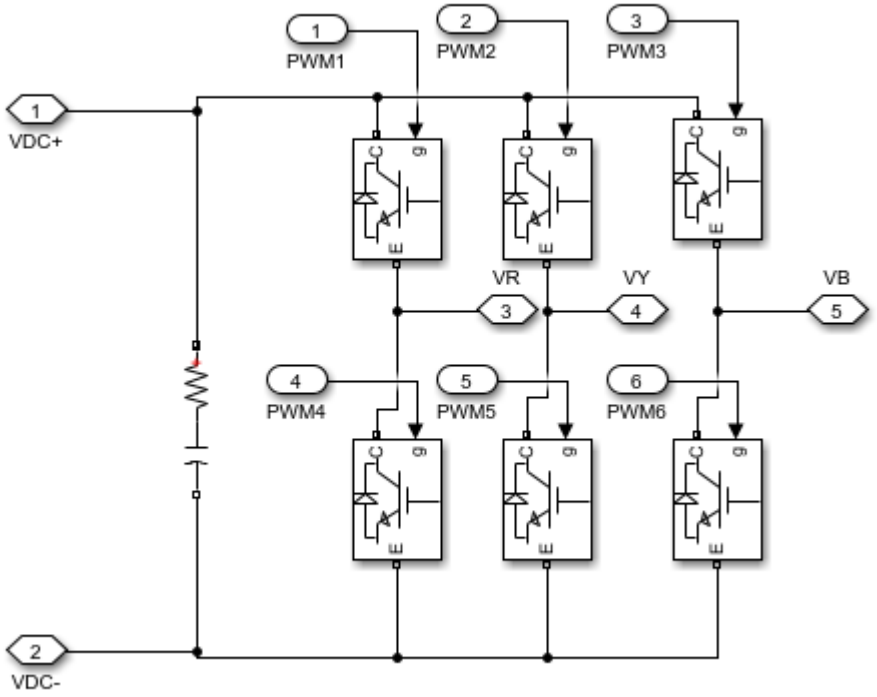

Figure 3.6: PWM Simulink

5. Modified ROGI control structure

Figure 3.7 shows the modeling of a modified ROGI control system derived by inserting the red lines blocks. The mathematical analysis of the updated ROGI control system is provided in Chapter 2.

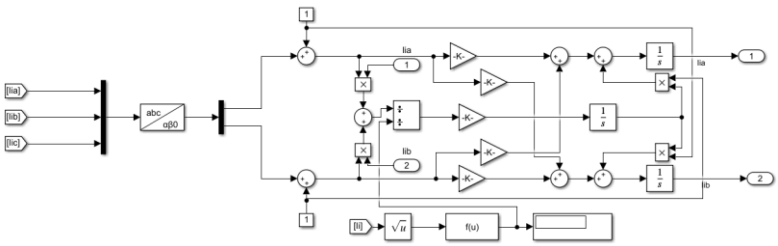

Figure 3.7: Modified structure of ROGI's control system

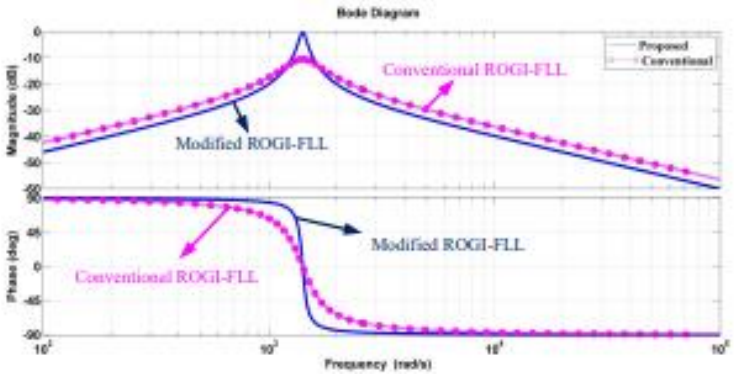

Figure 3.8: Modified ROGI-FLL stability comparison with regular ROGI

6. The proposed system's control schematic

We already explain calculation of Reference Current Generation in previous chapter, so now we will show the The proposed system's entire control schematic in figure 3.9.

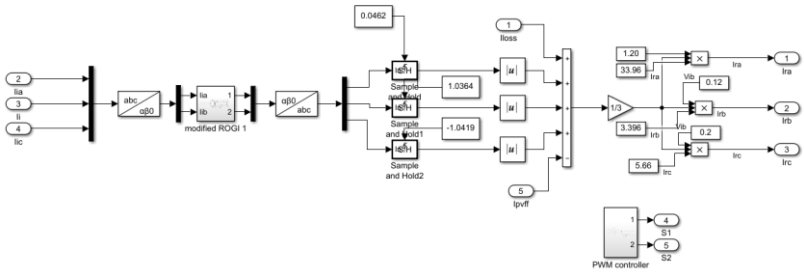

Figure 3.9: Simulation of the System

7. Loads

We use in this simulink simulation 3 external loads to effect on the current and voltage, we use (Motor Load, Linear Load, and non-linear Load). And we will presence all of them below in figures (3.10 , 3.11 , and 3.12),

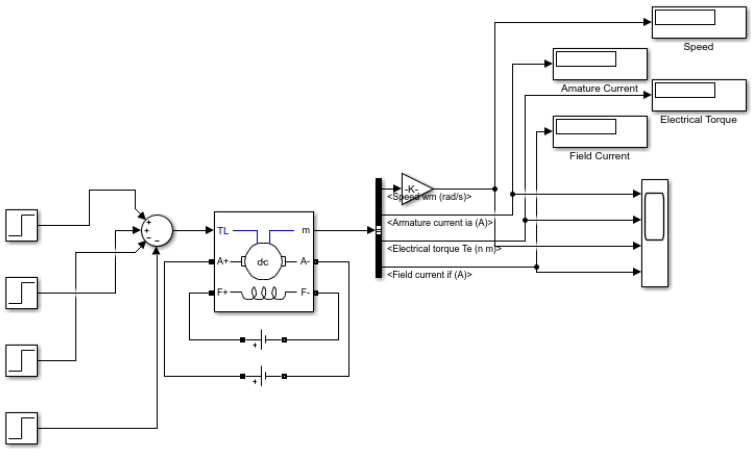

Figure 3.10: simulation of Motor Load

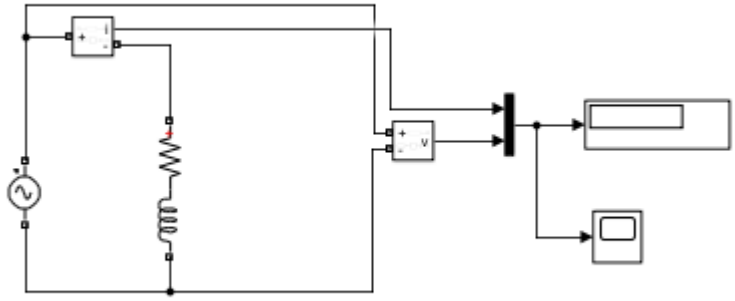

Figure 3.11: Linear Load's simulation

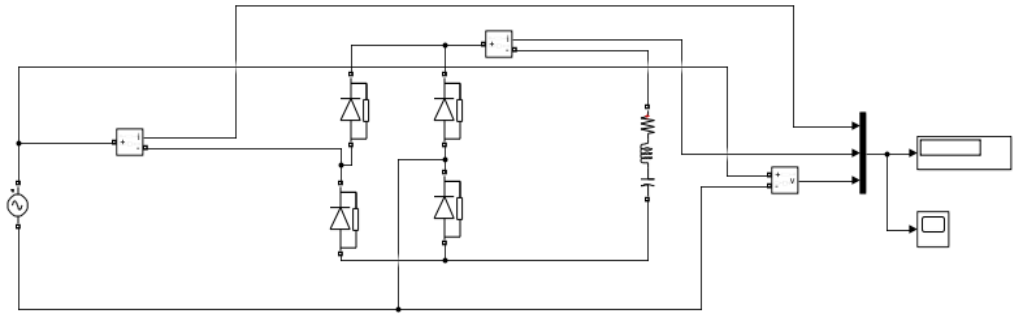

Figure 3.12: Simulation of Non-linear Load

8. Fuzzy Tuned PID

Traditional P, PI, and PID controllers have been proven to be ineffective in maintaining dc bus voltage stability under grid and load transient circumstances. A fuzzy tuned PID advanced control technique is proposed to compute PID

gains adaptively under transient situations to overcome this issue [25,26]. Figure 3.13 depicts the control diagram for the FLPID. The following is a discussion of the mathematical modeling of the FLPID controller:

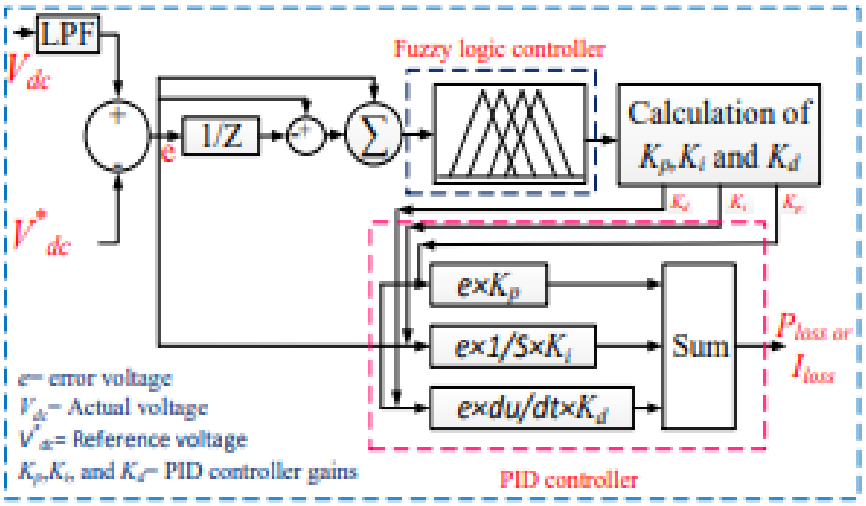

Figure 3.13: FLPID voltage controller schematic diagram

We can connect Fuzzy tuned PID to the PV array directly to effects on the whole system, as we will show in figure 3.14.

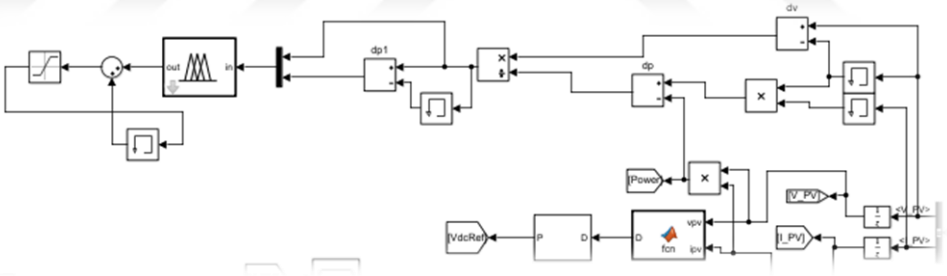

Figure 3.14: Fuzzy tuned PID simulink with MPPT

C. Analysis of Simulations

The Matlab/Simulink software platform was used to build the complete system. Tables 3.1 and 3.2, respectively, show the parameters used in the proposed system. The suggested MROGI-FLL approach is used to investigate a grid-connected PV system for power quality enhancement at the consumer terminals under steady-state, grid voltage dynamic, load removal, distorted supply voltage, and dynamic load status situations. A comparison of the MROGIFLL with traditional approaches is also performed, as shown in Tables 4.1 and 4.2, respectively.

Table 3.1: THE SYSTEM'S STANDARDS

Features	Modeling and Experimentation
Voltage on the grid (Vs)	230Volt
Power's Grid (Ps)	6kWatt
Frequency (f)	50 Hz
Impedance's Line (Zl)	R=0.01Ω, L=1.5mH
Interfacing inductor (Lapf)	2.2mH
Non-linear load (RL)	50Ω, 40mH
Load power (Pl)	6kWatt
DC bus capacitor (Cdc)	2200μF
Voltage on the DC bus	375Volt
α β gain in constituents (k)	0.707
Gain from cross coupling (k 0)	-64
Lambda (λ)	12791
Frequency estimates (ω')	2*π*f

Table 3.2: THE SYSTEM'S STANDARDS

Features	Modeling and Experimentation	
(P_{pv})	2kWatt	1.6kWatt
(G)	1000 W/m2	1000 W/m2
Open-circuit-voltage(V_{oc})	210Volt	200Volt
Short-circuit-current (I_{sc})	10.85A	8.96A
Max-PV-voltage (V_{mp})	190Volt	190Volt
Max-PV-current (I_{mp})	10.52A	8.42A
DC-link-voltage (V_{dc})	375Volts	375Volts
DC-link-current (I_{dc})	4.3A	4.3A
No. of series modules (NS)	11	6
No. of parallel modules (NP)	3	1

IV. CONCLUSION AND DISCUSSION OF THE RESULTS

In this chapter, we will look at the simulation results and compare them to the results of other systems. After that, we will offer a final evaluation at the conclusion of the section. Firstly, we will see the results of Incremental Conductance (INC).

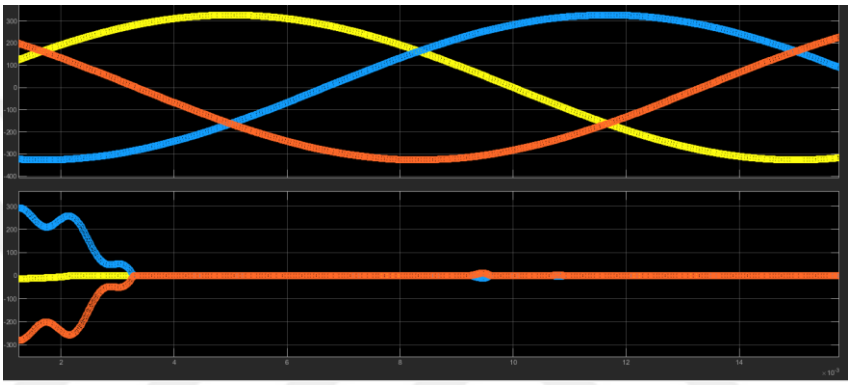

Figure 4.1: Current and Voltage with one external load

As we see in the figure 4.1, the current has a waveform and has a minimum value -380 A while the maximum is 380 V. On the other hand, the voltahe took a fork shape in the beginning then a straight line. The maximum voltage was 300 V and the minimum was -300 V.

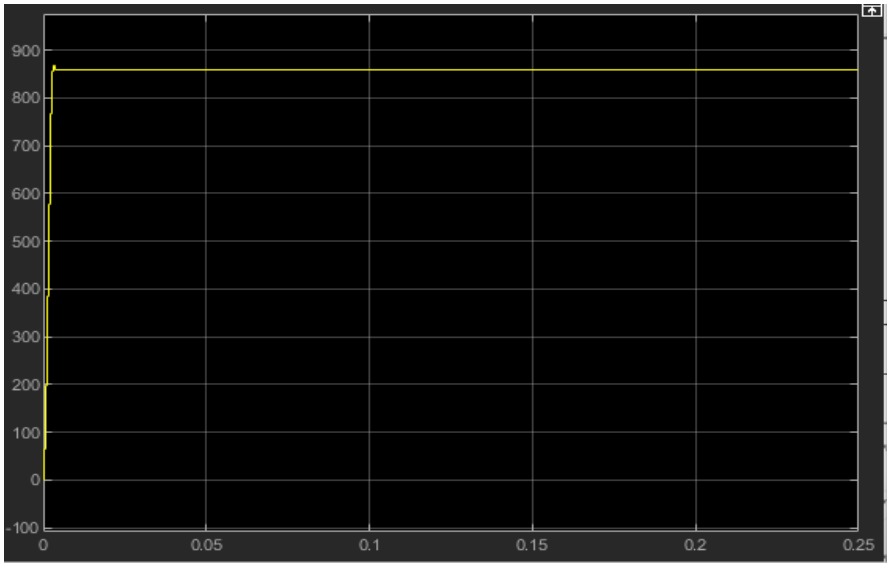

Figure 4.2: Voltage of PV with one external load

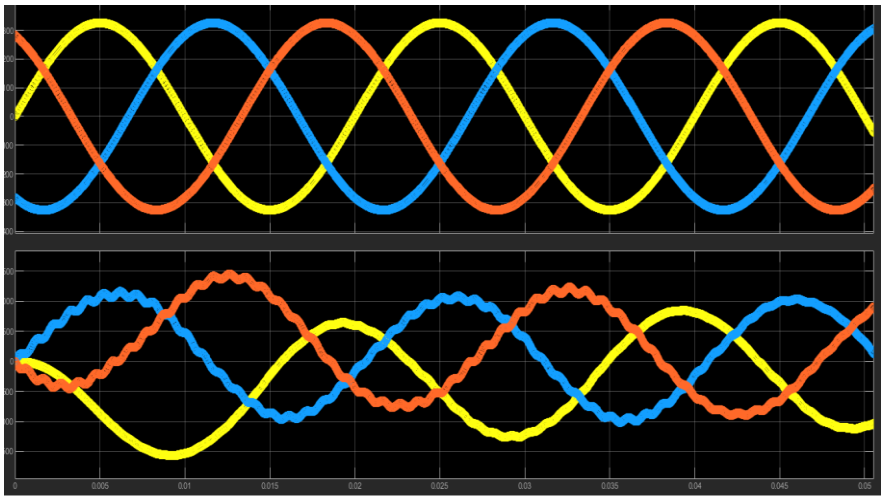

Figure 4.3: Current and Voltage with two external load

In this figure, we can see that the results is better when we added an external load to the system. Because the external load will effect on the voltage and current which means changing in the power of the system.

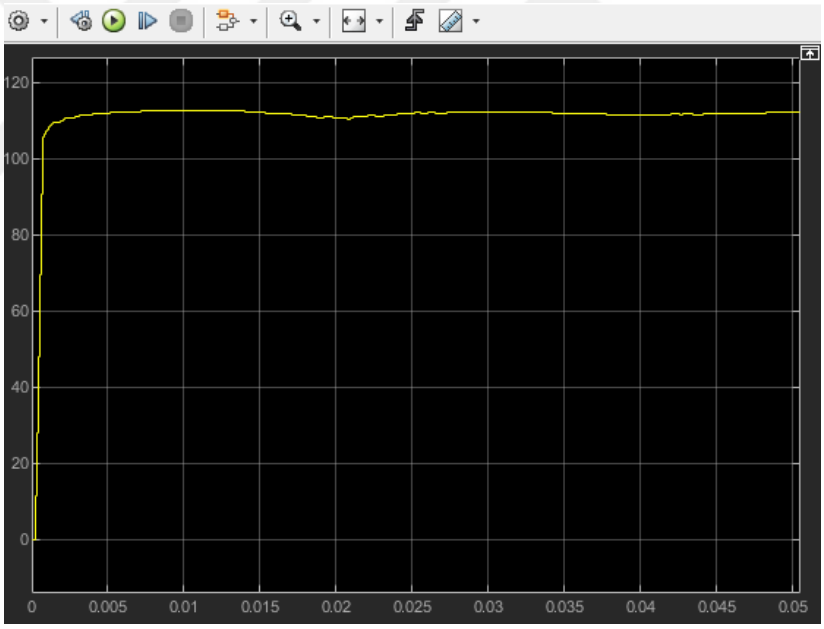

Figure 4.4: Voltage of PV with two external load

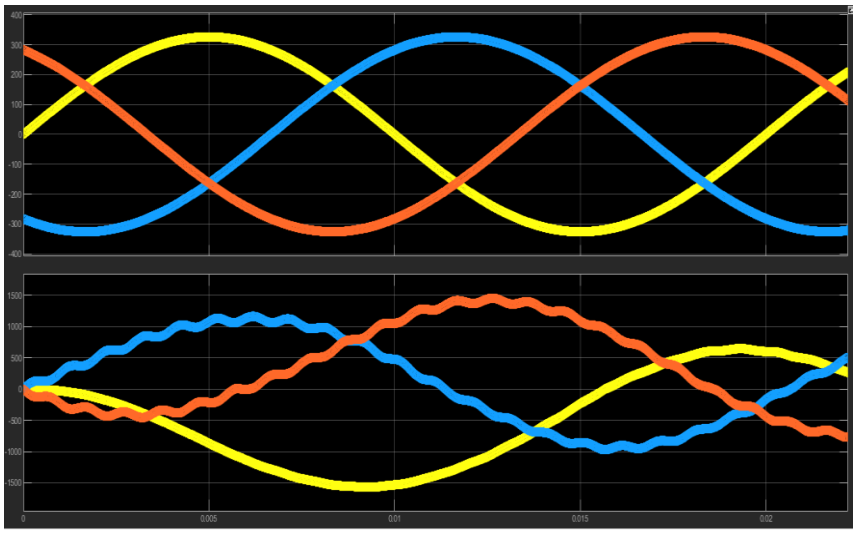

Figure 4.5: Current and Voltage with three external load

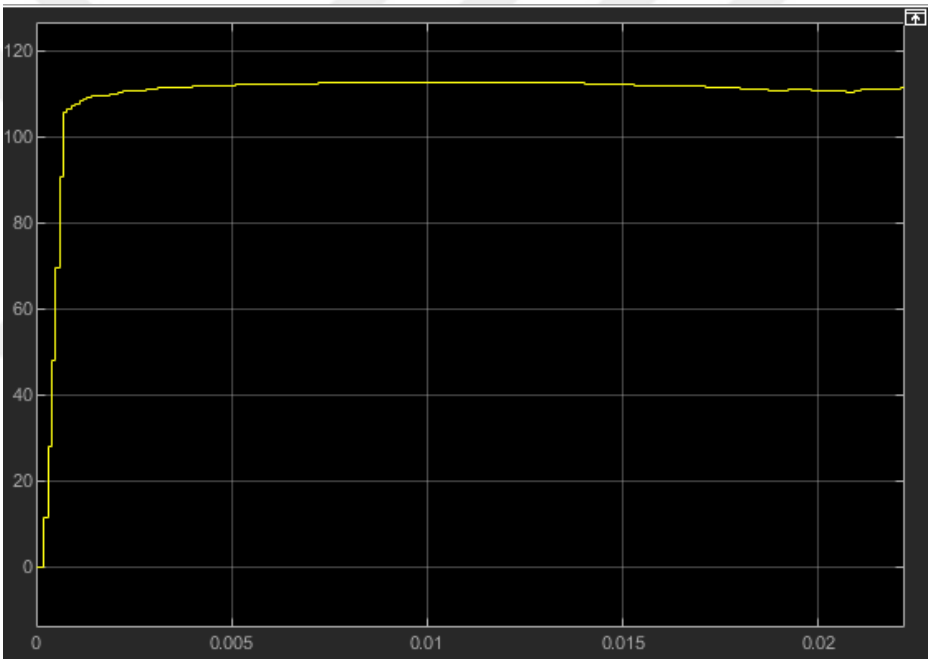

Figure 4.6: Voltage of PV with three external load

Now, we will present the results of P&O MPPT below;

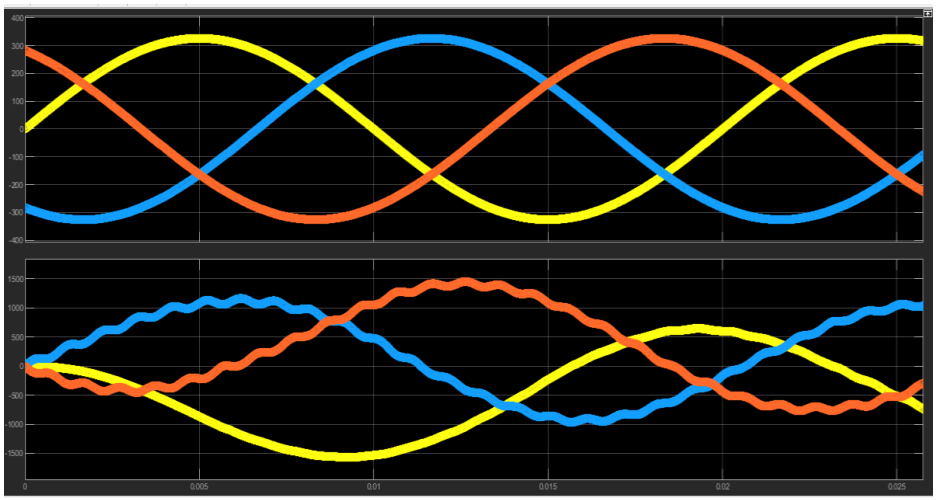

Figure 4.7: Current and Voltage with one external load

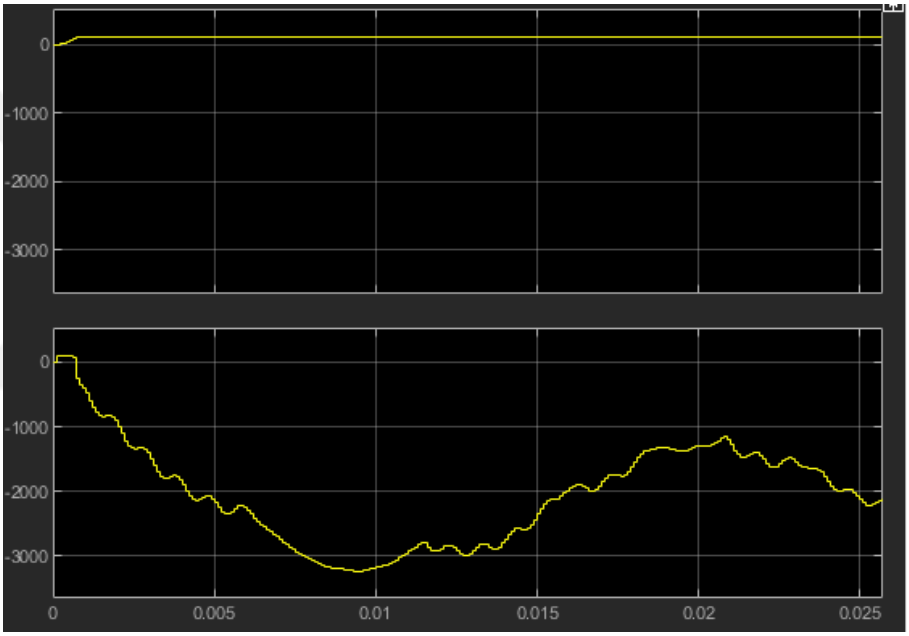

Figure 4.8: Current and Voltage with one external load

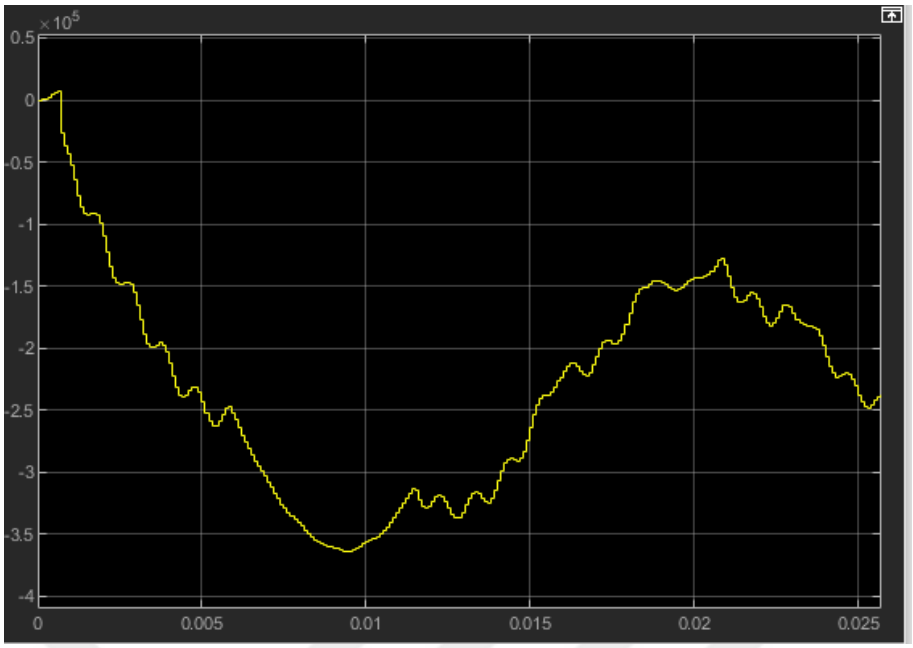

Figure 4.9: The power of the system

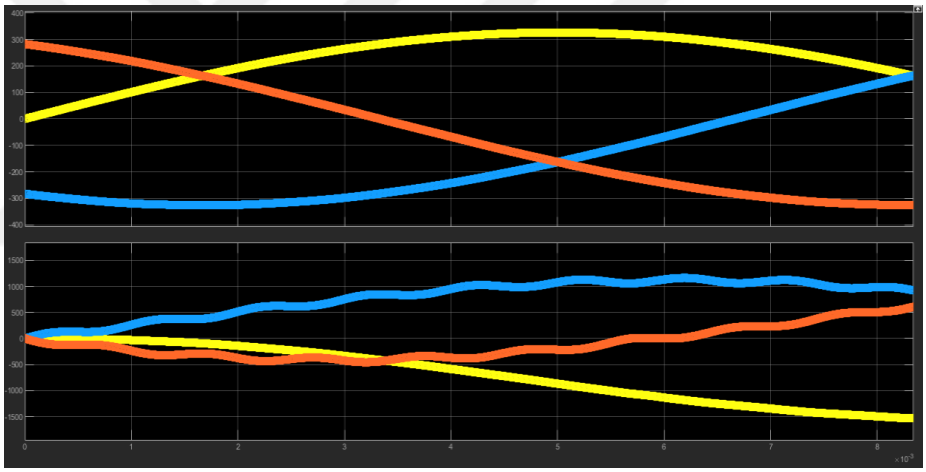

Figure 4.10: Current and Voltage with two external load

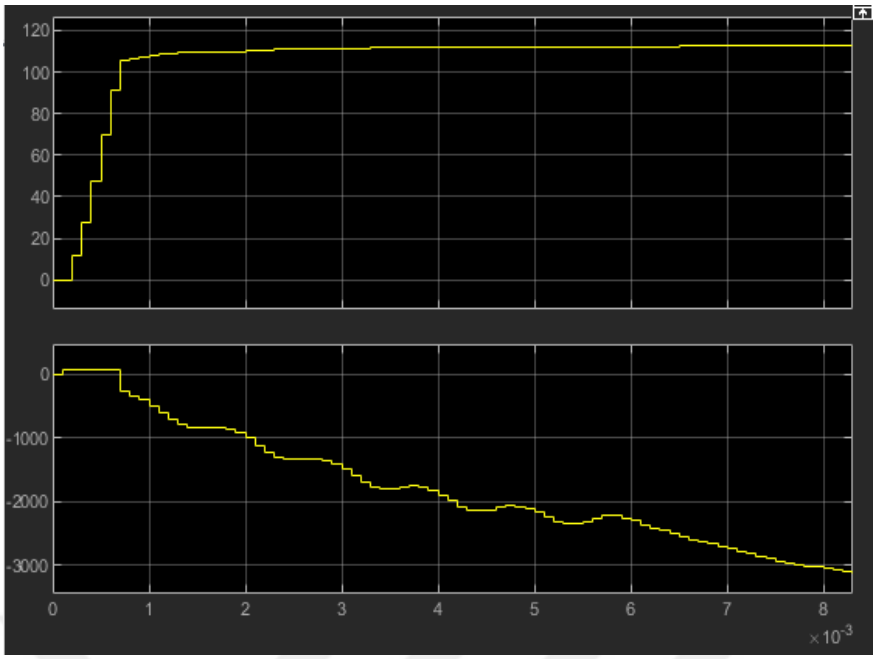

Figure 4.11: Current and Voltage with two external load

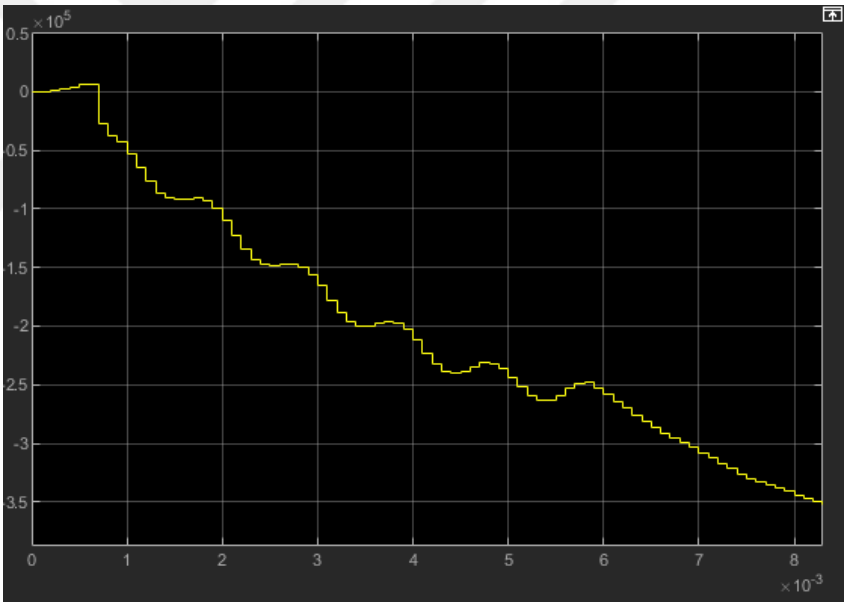

Figure 4.12: The Power of the system

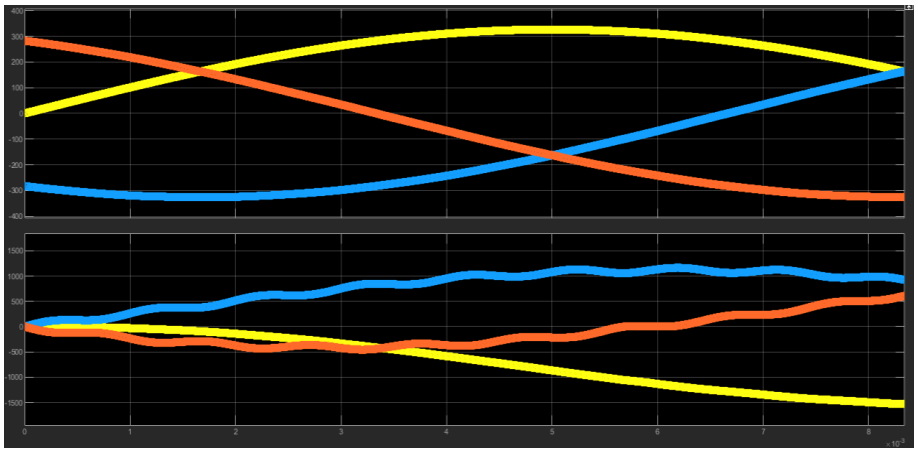

Figure 4.13: Current and Voltage with three external load

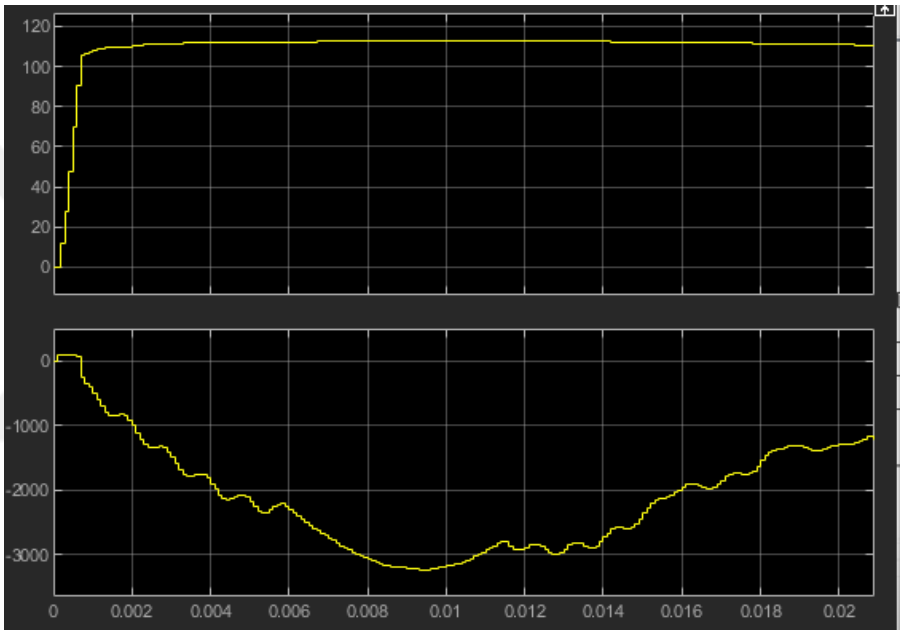

Figure 4.14: Current and Voltage with three external load

Figure 4.15: Power of the system

Now, we will remove the Adaptive dc voltage controller and replace it with Fuzzy tuned PID and the results will presence below;

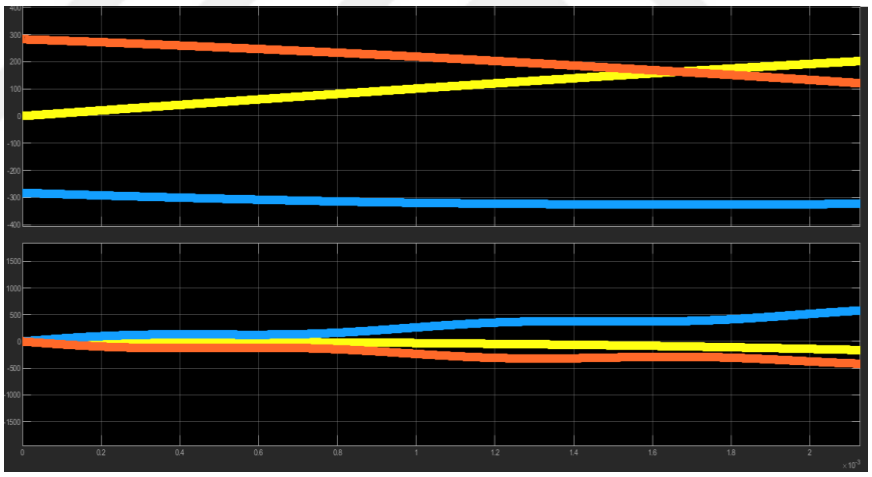

Figure 4.16: Current & Voltage with Fuzzy tuned PID with P&O

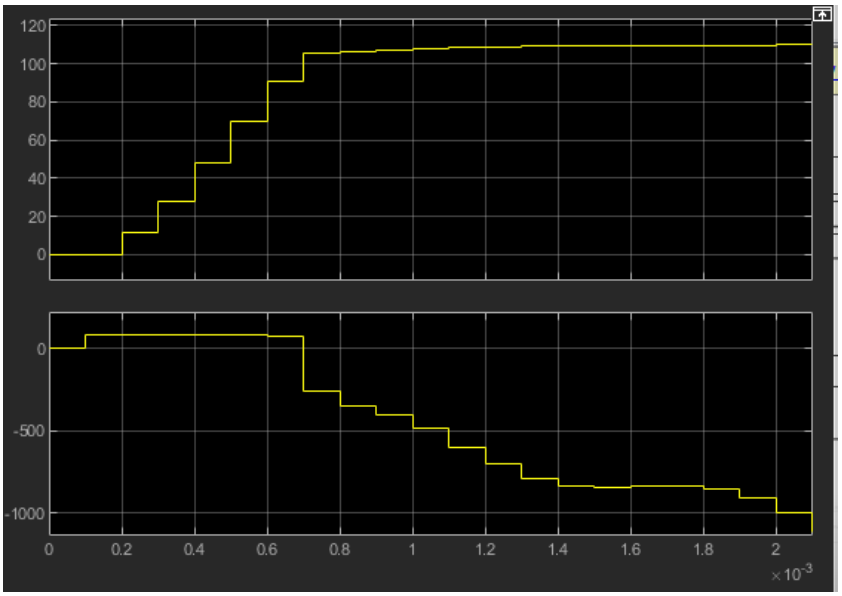

Figure 4.17: Current & Voltage with Fuzzy tuned PID with P&O

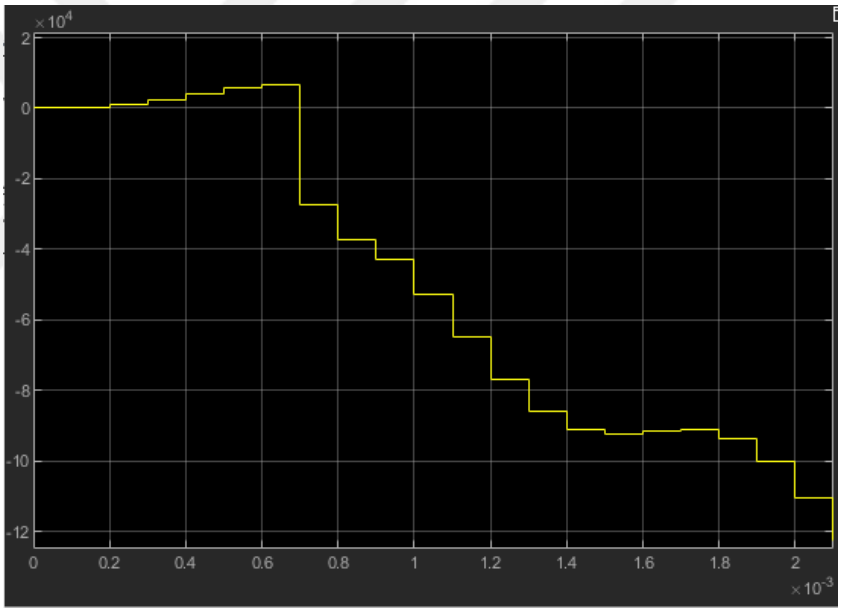

Figure 4.18: Power of the system with Fuzzy tuned PID with P&O

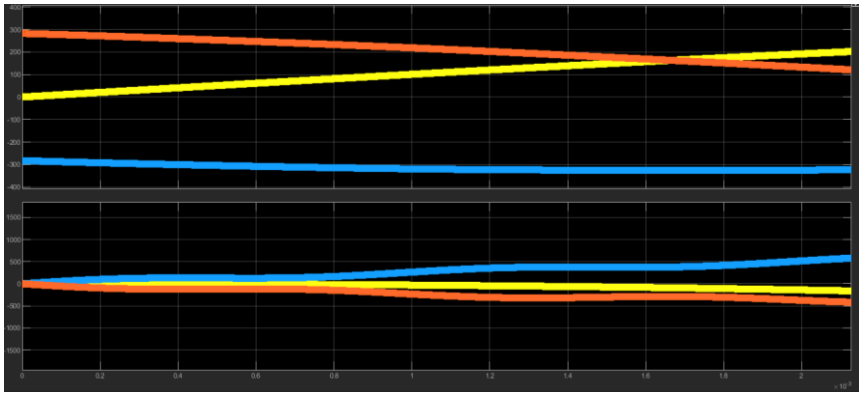

Figure 4.19: Current & Voltage with Fuzzy tuned PID with P&O

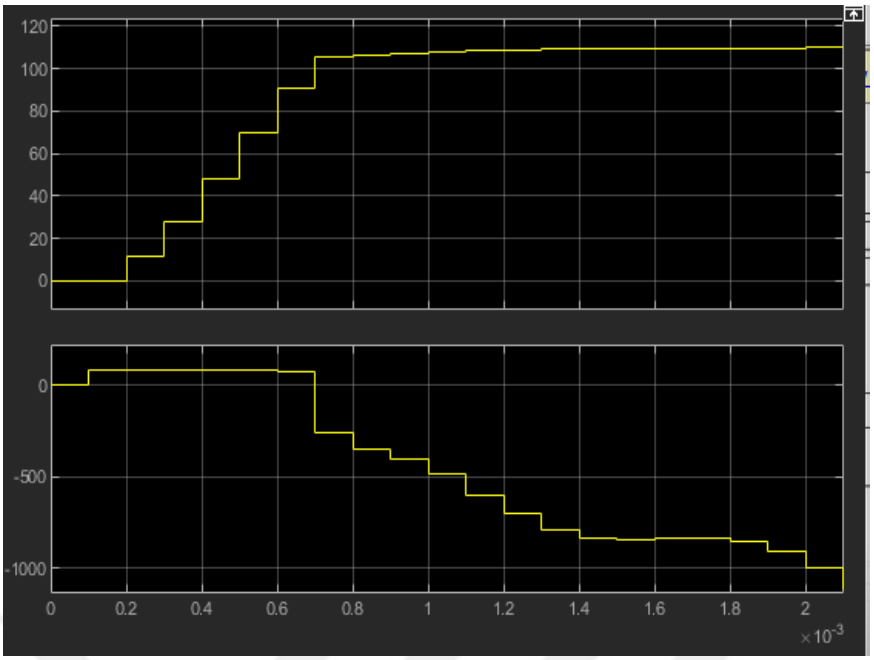

Figure 4.20: Current & Voltage with Fuzzy tuned PID with P&O

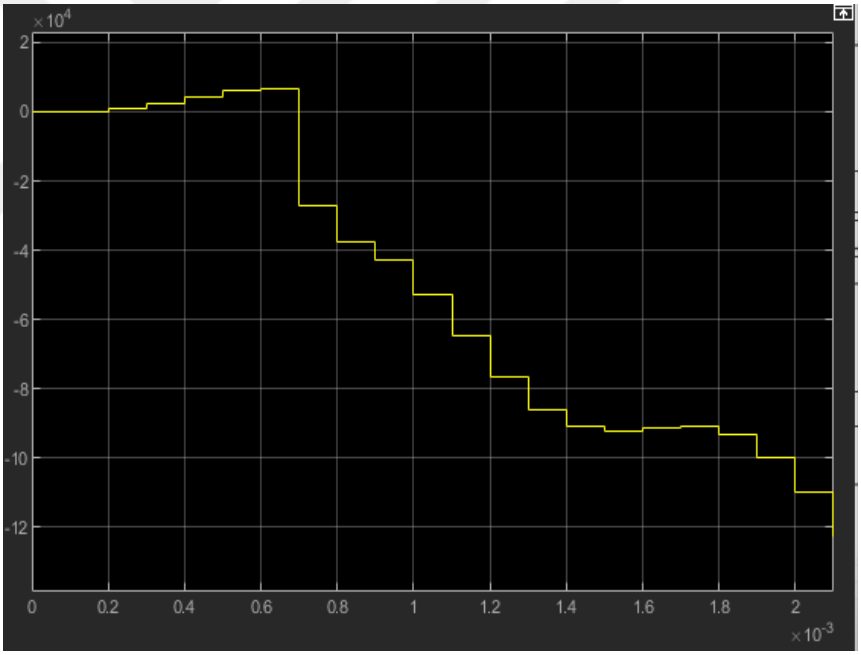

Figure 4.21: Power of the system with Fuzzy tuned PID with P&O

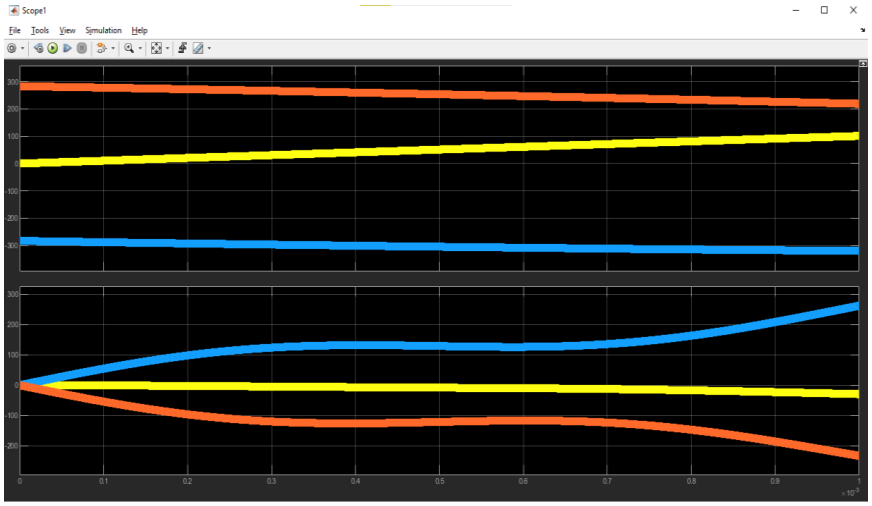

Figure 4.22: Current & Voltage with Fuzzy tuned PID with P&O

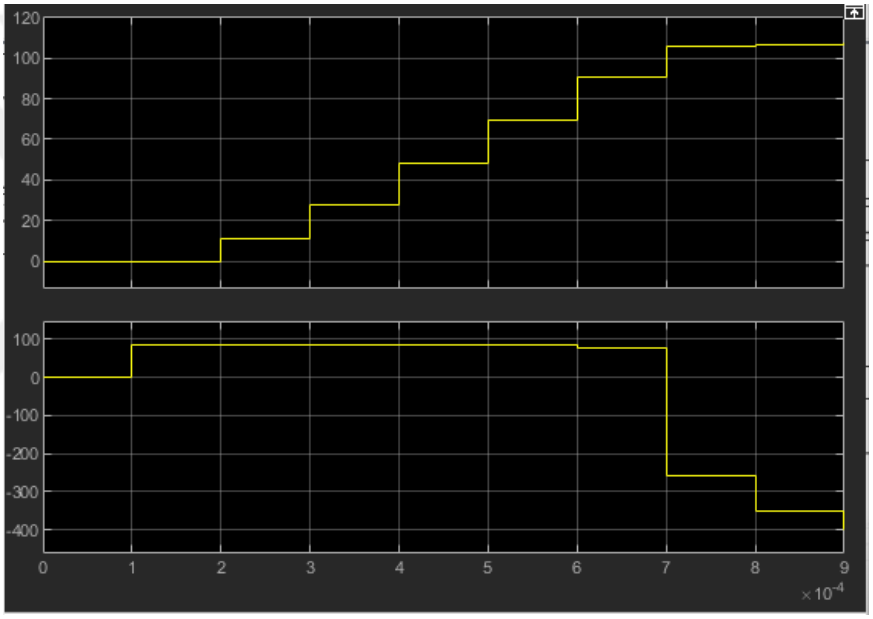

Figure 4.23: Current & Voltage with Fuzzy tuned PID with P&O

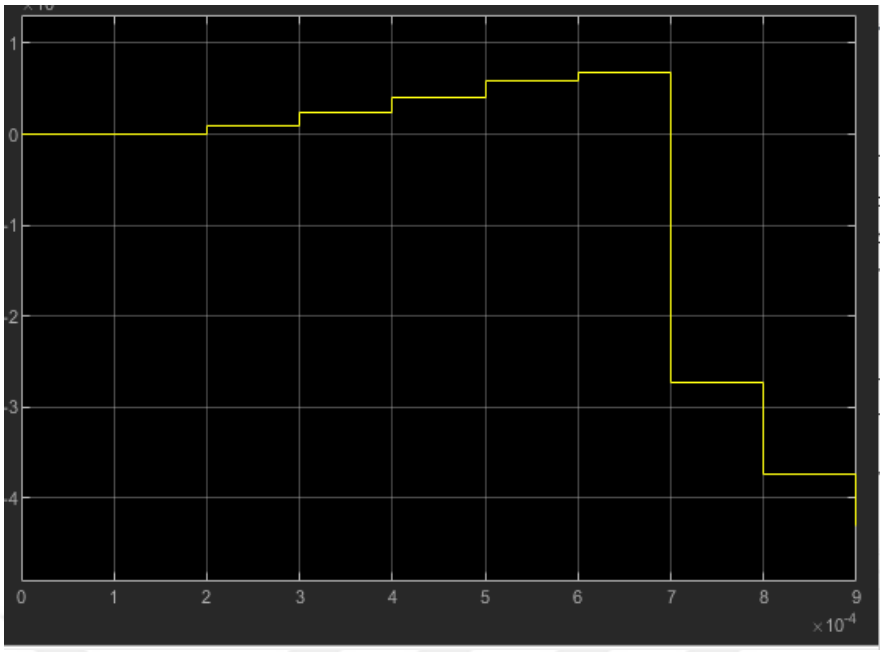

Figure 4.24: Power of the system with Fuzzy tuned PID with P&O

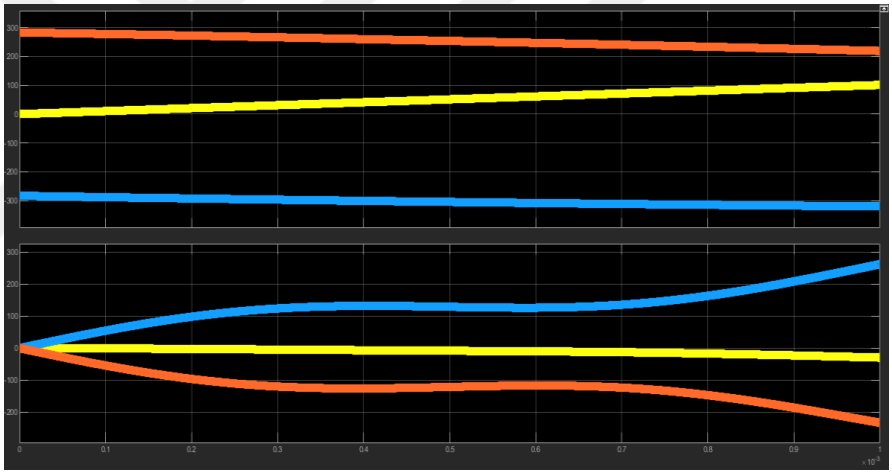

Figure 4.25: Current & Voltage of the system with Fuzzy tuned PID with INC

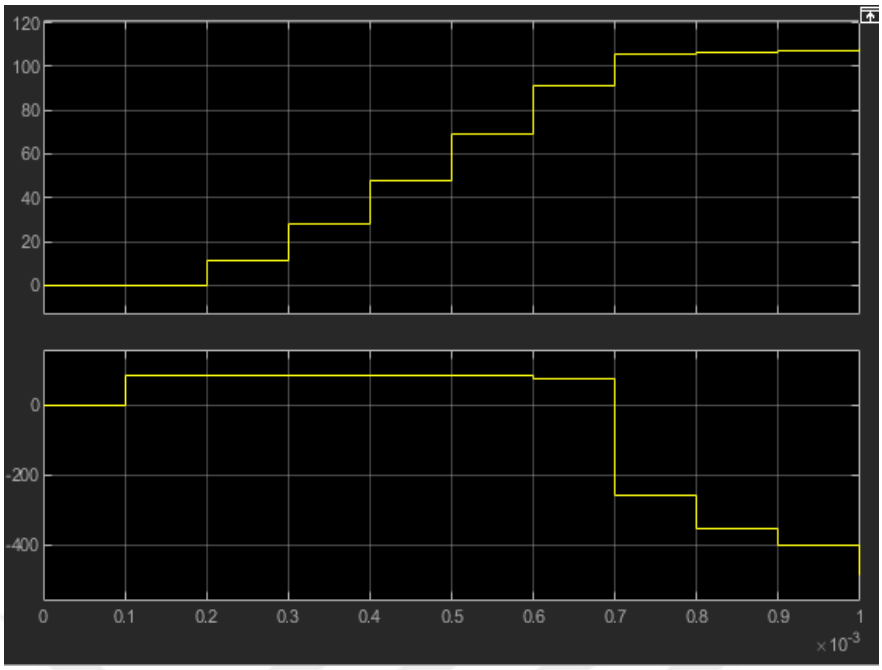

Figure 4.26: Current & Voltage of the system with Fuzzy tuned PID with INC

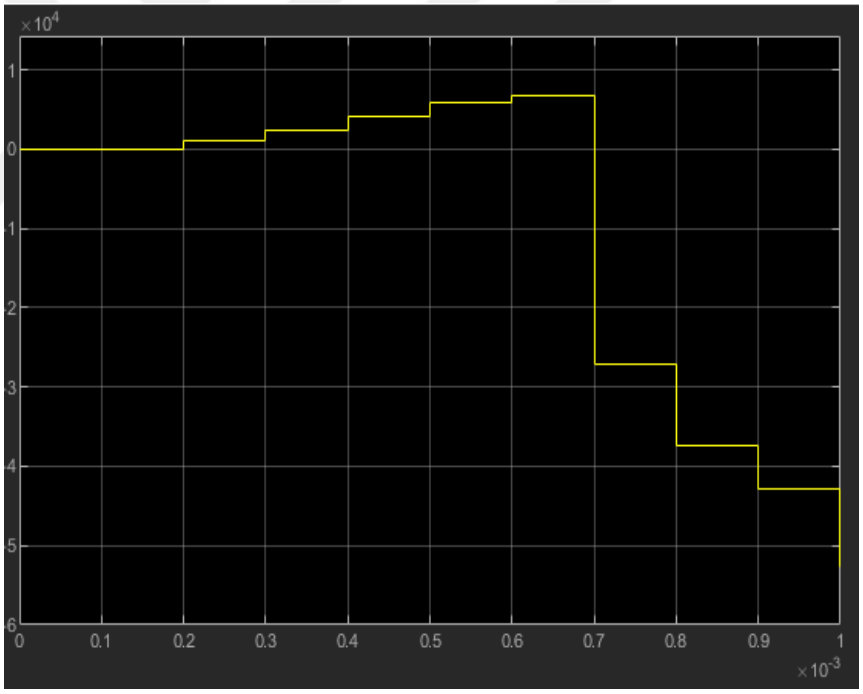

Figure 4.27: Power of the system with Fuzzy tuned PID with INC

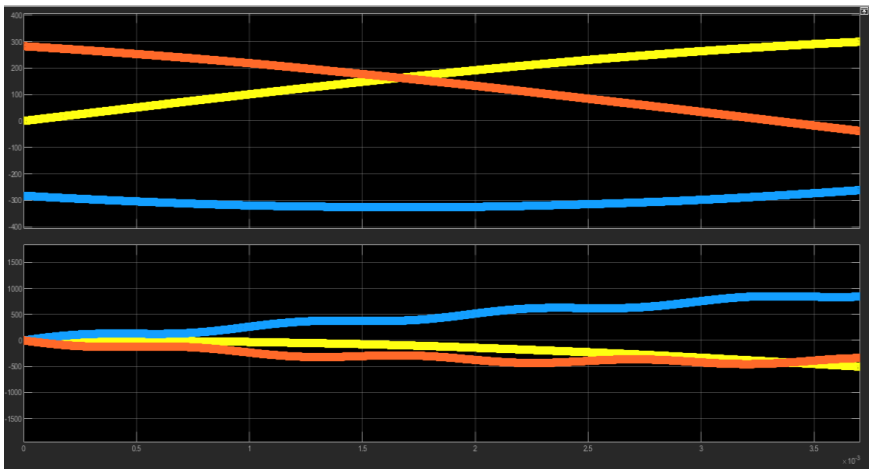

Figure 4.28: Current & Voltage of the system with Fuzzy tuned PID with INC

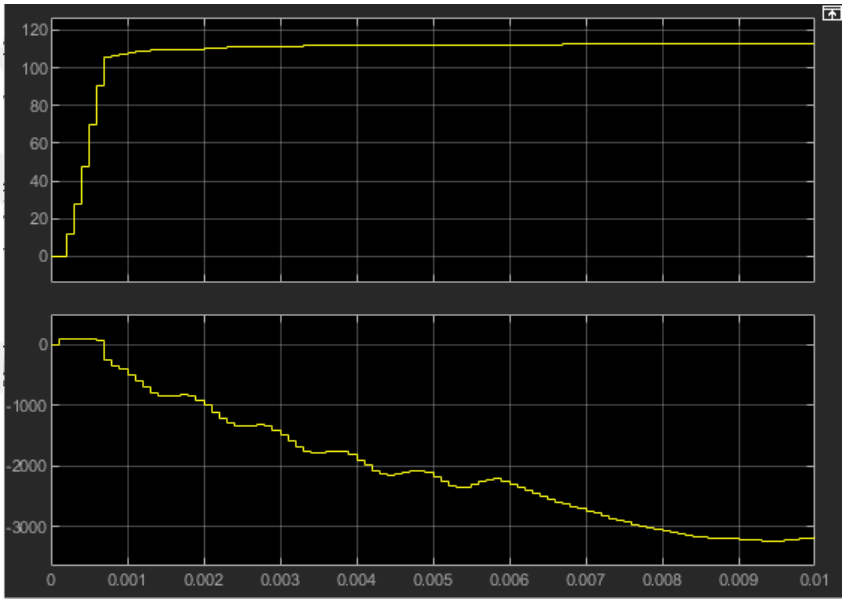

Figure 4.29: Current & Voltage of the system with Fuzzy tuned PID with INC

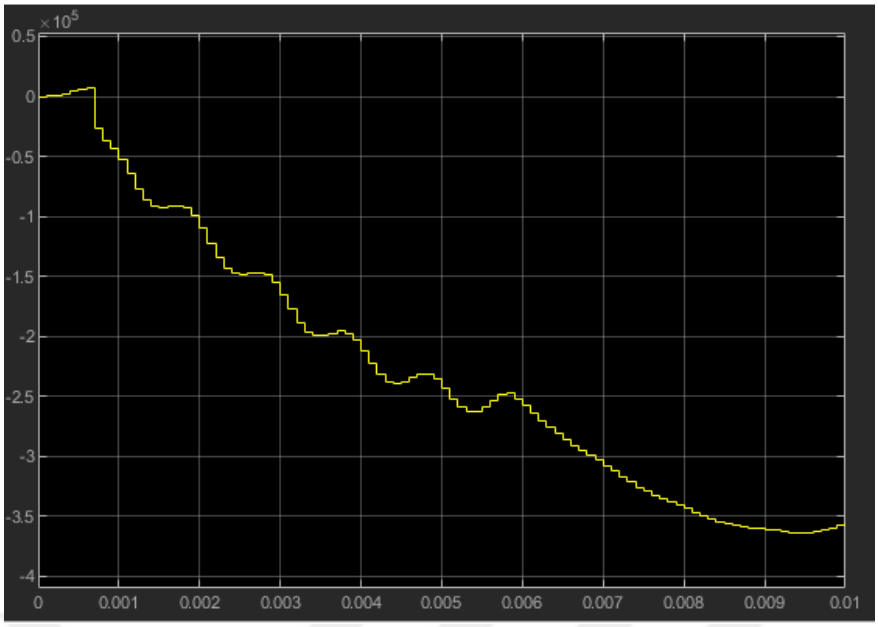

Figure 4.30: Power of the system with Fuzzy tuned PID with INC

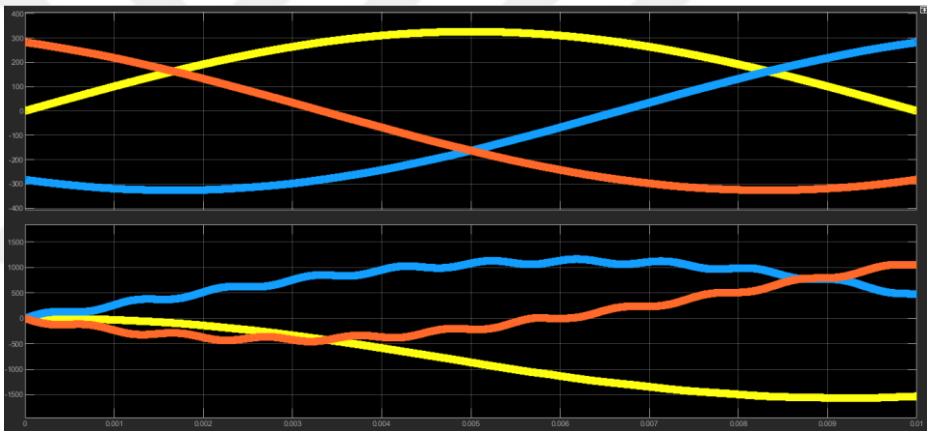

Figure 4.31: Current & Voltage of the system with Fuzzy tuned PID with INC

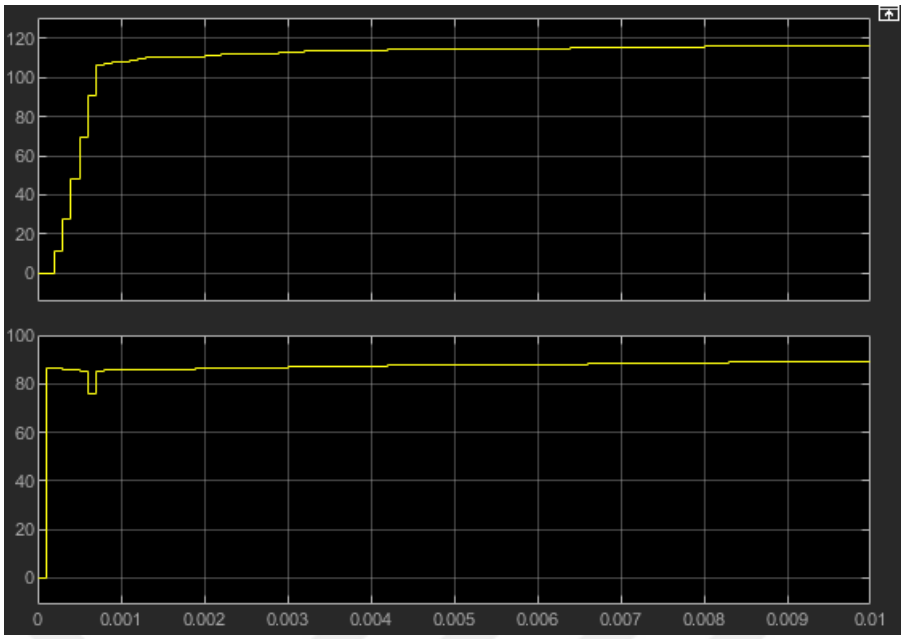

Figure 4.32: Current & Voltage of the system with Fuzzy tuned PID with INC

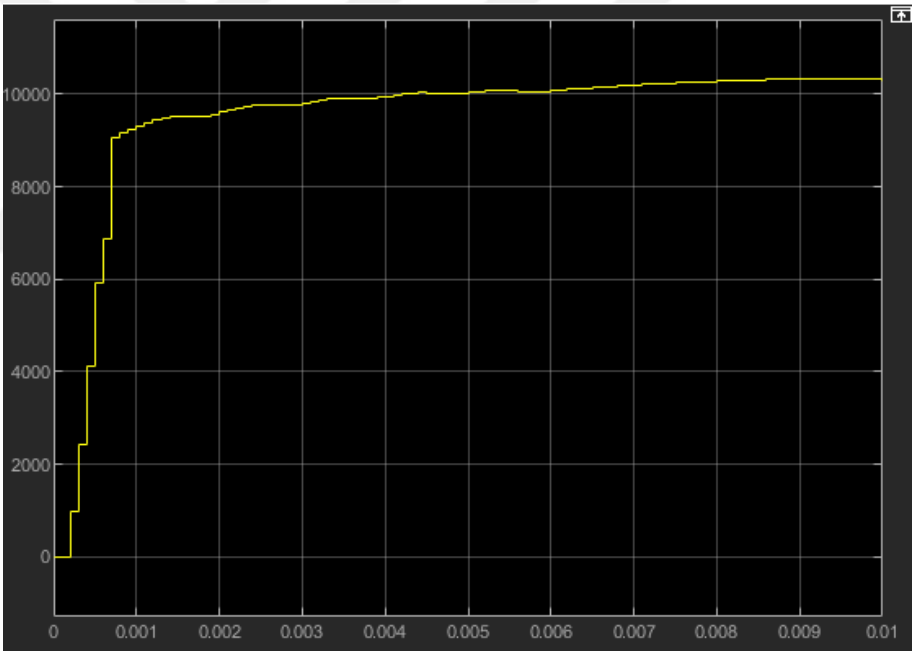

Figure 4.33: Power of the system with Fuzzy tuned PID with INC

For adding the Fuzzy to the system, we will add some specials block to the system.

MEMORY: To hold the previous value, and we used more than one memory.

MUX: which means multiplexer, and its a block allowed us in order to choose from a variety of analog and digital incoming signal and send the chosen input

to a signal is applied. Example, we have 4 input and we need only one output, in that case we will use the mux to make 1 output with 4 different input.

Now we will compare between the P&O, IC MPPT with Fuzzy tuned PID. As we shown previous, we can see that the P&O and IC gave us better results for the system and we can make more analysis on it. Also it's more clearly and easier to use the adaptive dc vpltage controller than the fuzzy.

Now we will show the comparison between Adaptive dc voltage controller and Fuzzy tuned PID.

A. Case I

Incremental Conductance with adaptive dc volttage controller and with fuzzy tuned PID.

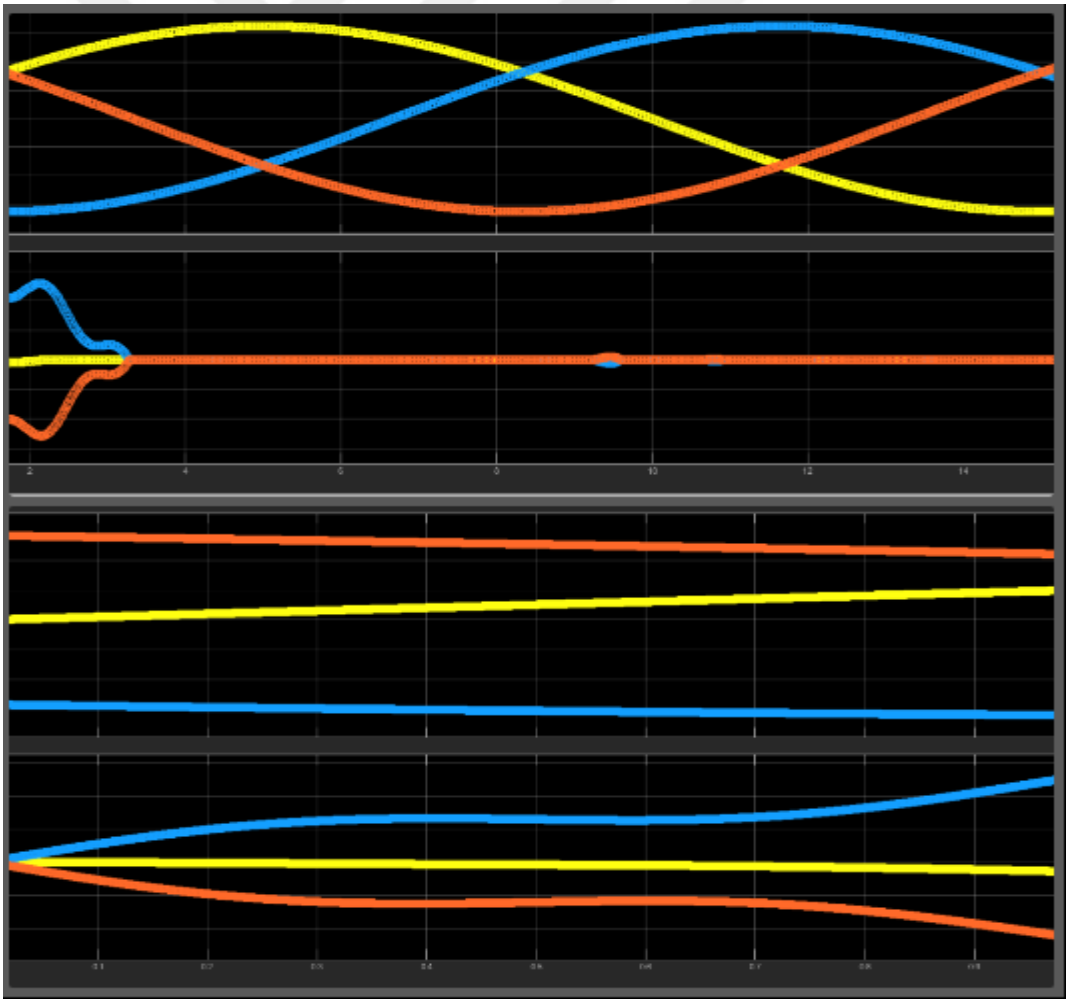

Figure 4.34: IC MPPT with adaptive dc volttage controller - IC MPPT with Fuzzy PID

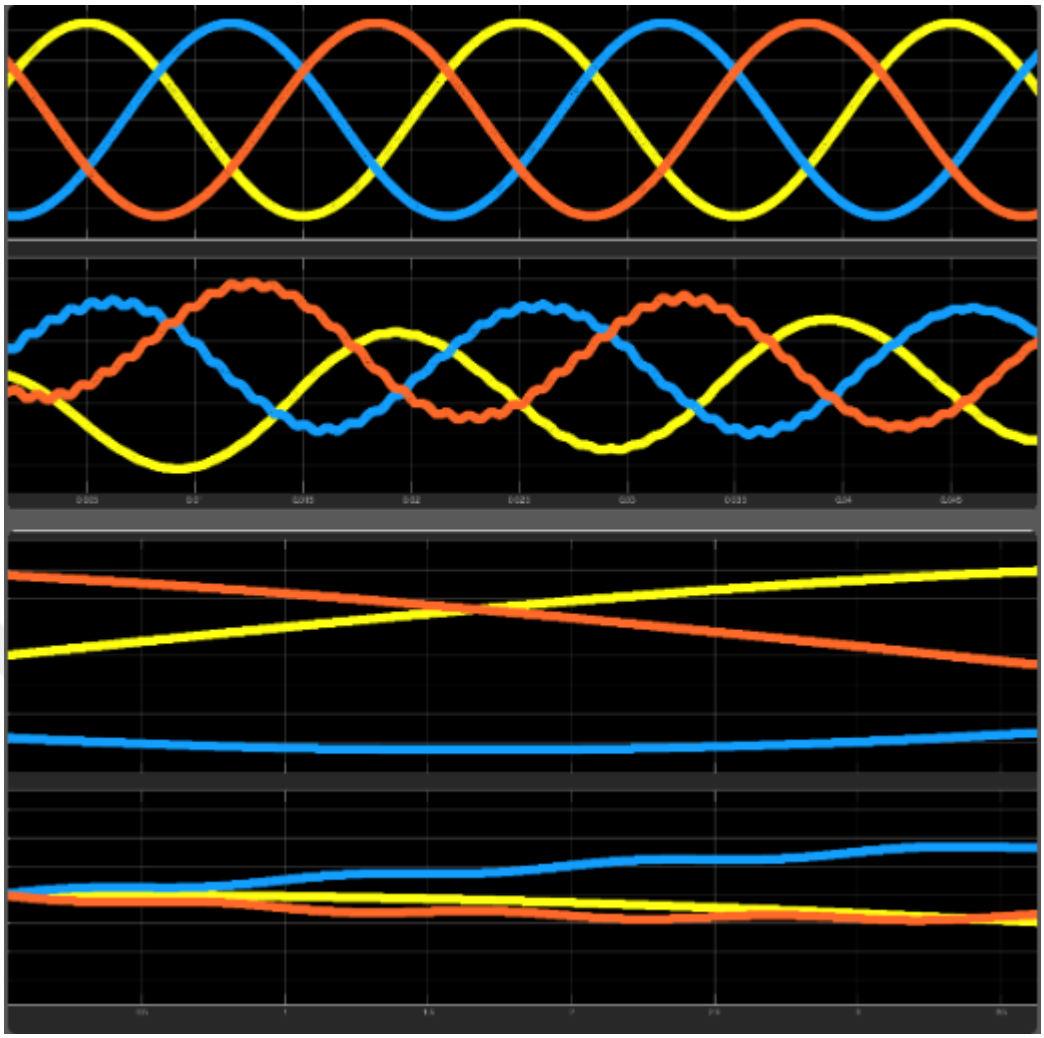

Figure 4.35: IC MPPT with adaptive dc volttage controller - IC MPPT with Fuzzy PID

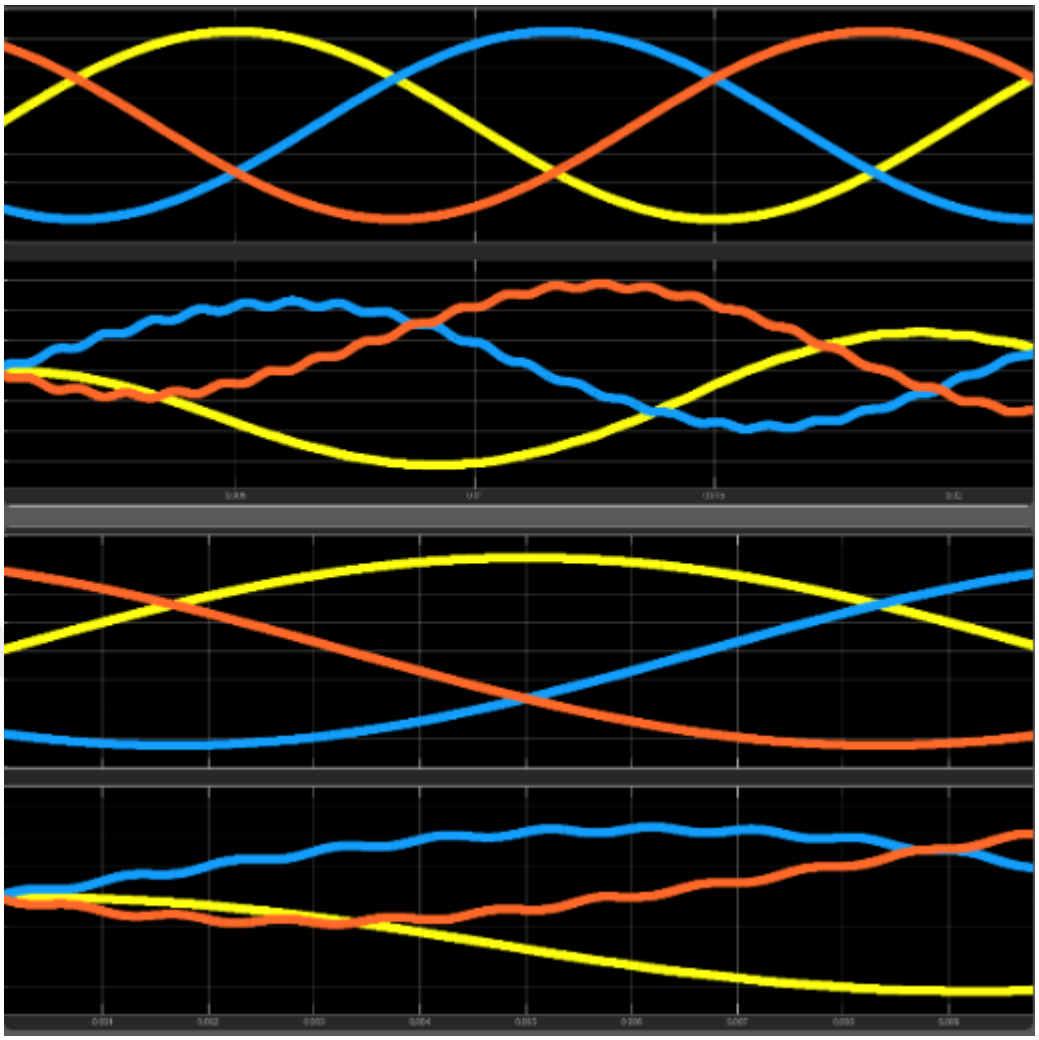

Figure 4.36: IC MPPT with adaptive dc volttage controller - IC MPPT with Fuzzy PID

B. Case II

Peninsula and Oriental with adaptive dc volttage controller and with fuzzy tuned PID.

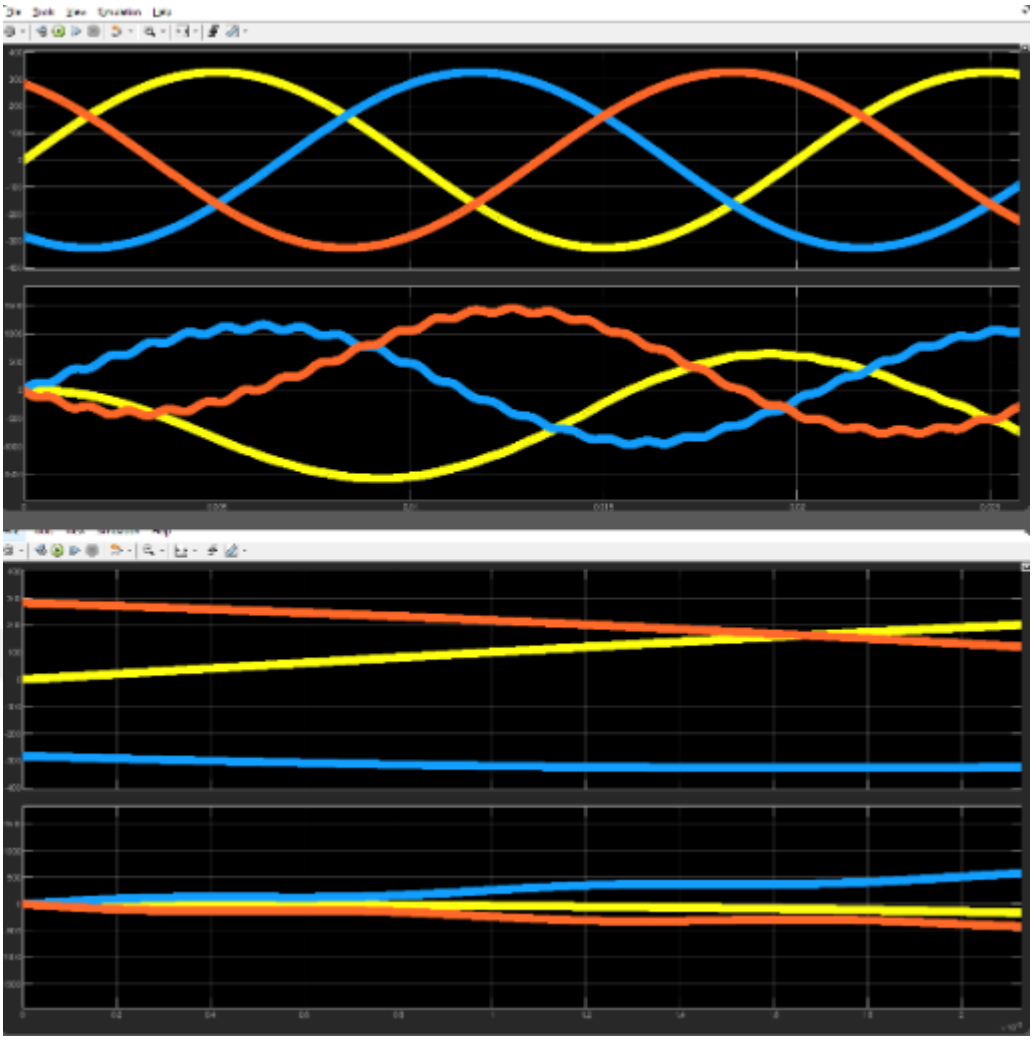

Figure 4.37: P&O MPPT with adaptive dc volttage controller - P&O MPPT with Fuzzy PID

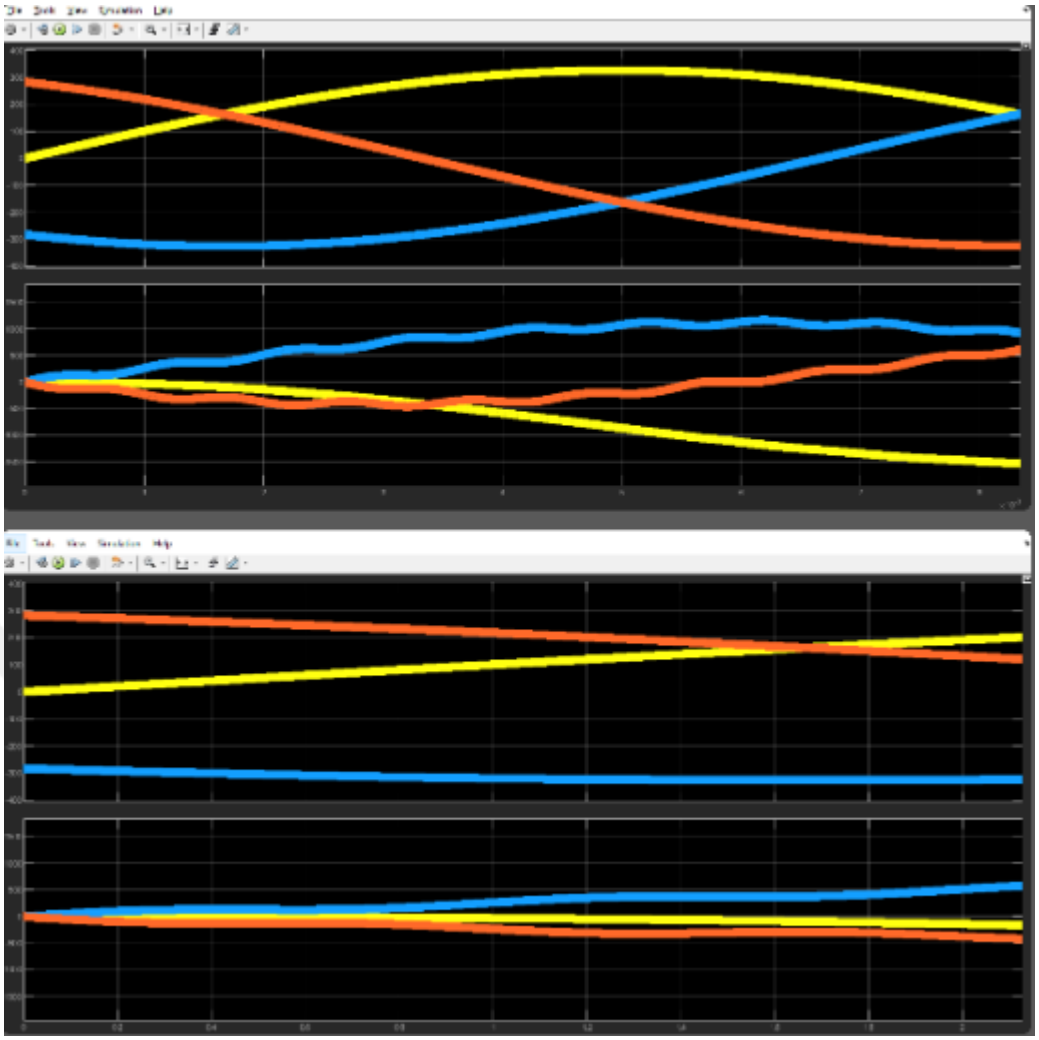

Figure 4.38: P&O MPPT with adaptive dc volttage controller - P&O MPPT with Fuzzy PID

C. Case III: Condition of balanced supply voltages

The corresponding experimental results are shown in Figure 4.39 to 4.40. Display the grid as well as the recommended control parameters. Without compensation, the supply current THD is 26.452 percent, while with compensation, it is lowered to 2.261 percent. Figure 3.39 shows that the current is obviously sinusoidal and at unity power factor.

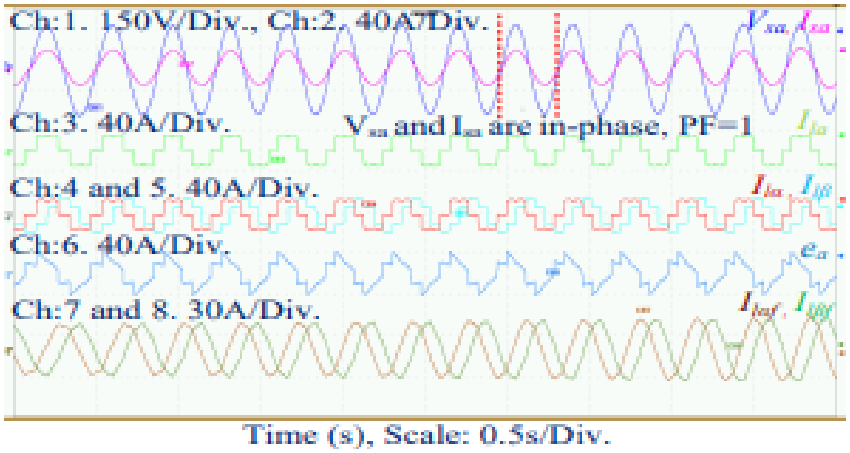

Figure 4.39: Grid properties are shown below steady-state situation

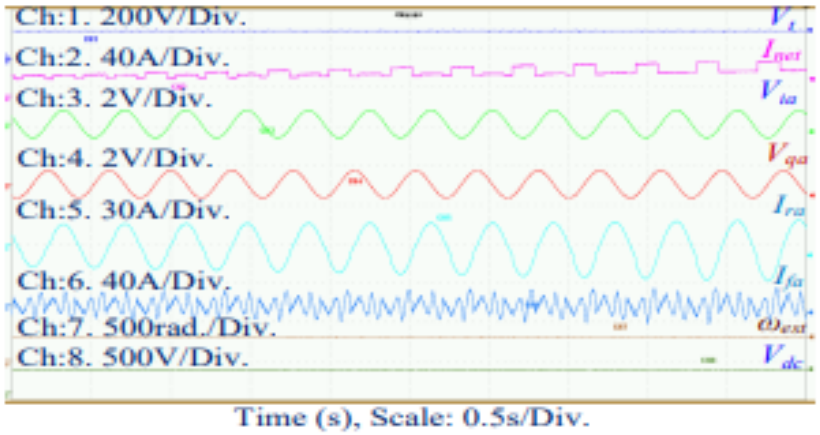

Figure 4.40: Control properties in a steady-state situation

D. Case IV: a problem with the system's voltage balance

The performance of the proposed grid-friendly PV-connected SAPF system under imbalanced voltages in the PCC voltage is also tested. Using the three single-phase variacs, the magnitude of each phase has altered a percentage of 10% raised and lowered of the nominal grid voltage for the imbalanced grid voltage situations.

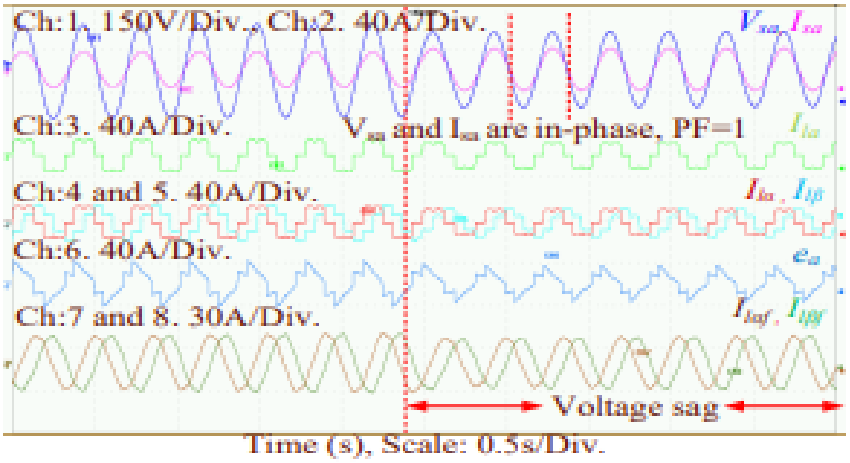

Figure 4.41: Grid characteristics when there is a voltage sag

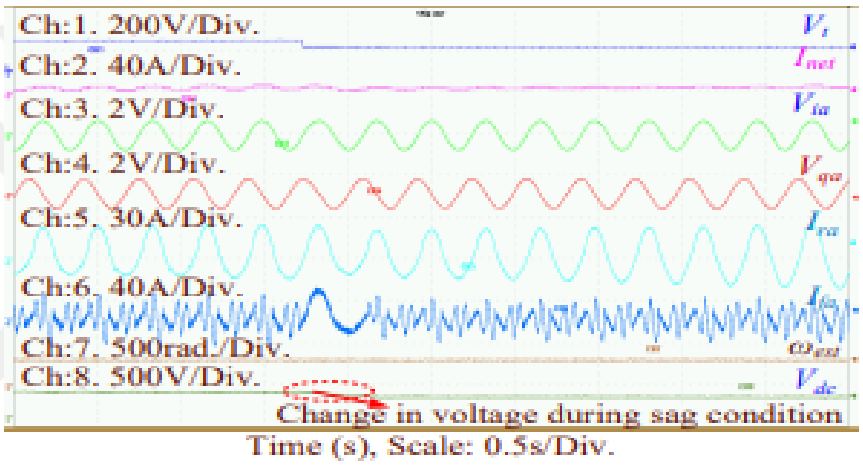

Figure 4.42: Control characteristics in the event of a voltage sag

Figure 4.43, is used to display the grid voltage, grid current, load-current error current (FCE), and grid error current (IEC). Fig. 16 shows that the shunt-connected system generates a balanced grid current at unbalanced grid voltages. Grid-current references are calculated by multiplying the average load current by the unit templates, according to the planned control system. Unit templates and average load current do not change under any load or grid situations. As an example, consider the control group's findings in Figure 4.43.

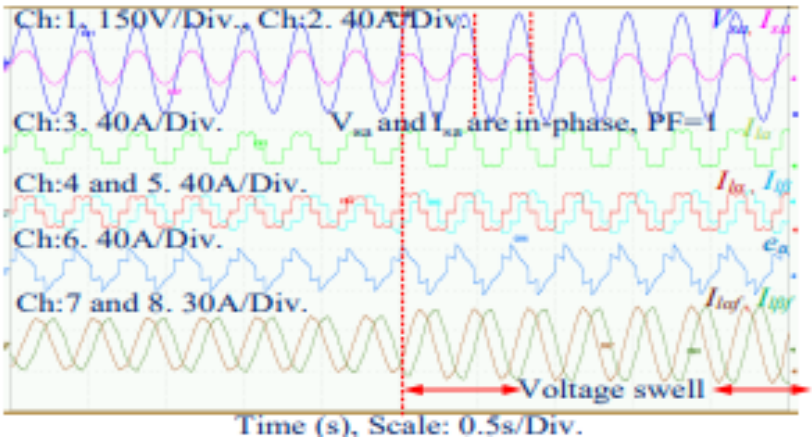

Figure 4.43: Under voltage swell conditions, the grid's characteristics

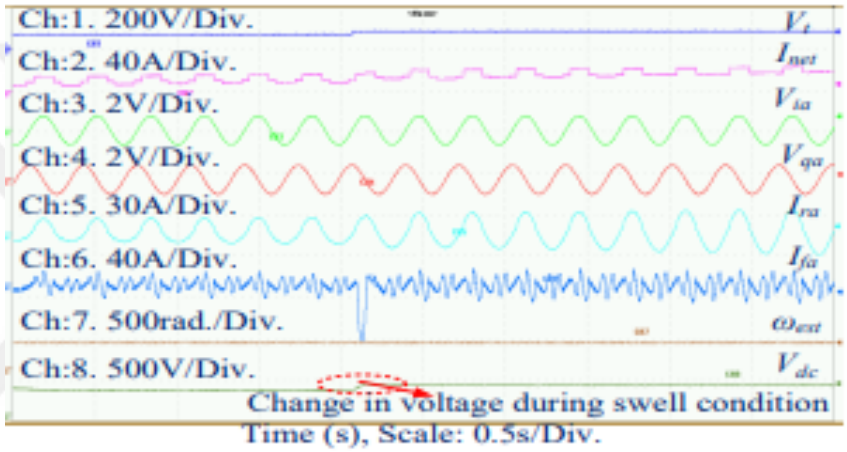

Figure 4.44: Characteristics of the control system in the presence of voltage swell

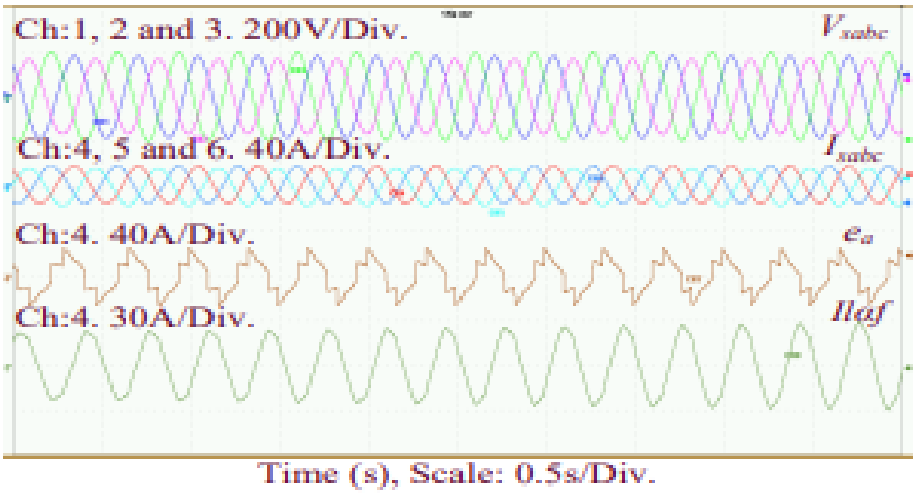

Figure 4.45: Characteristics of the grid when the voltage is out of balance voltages

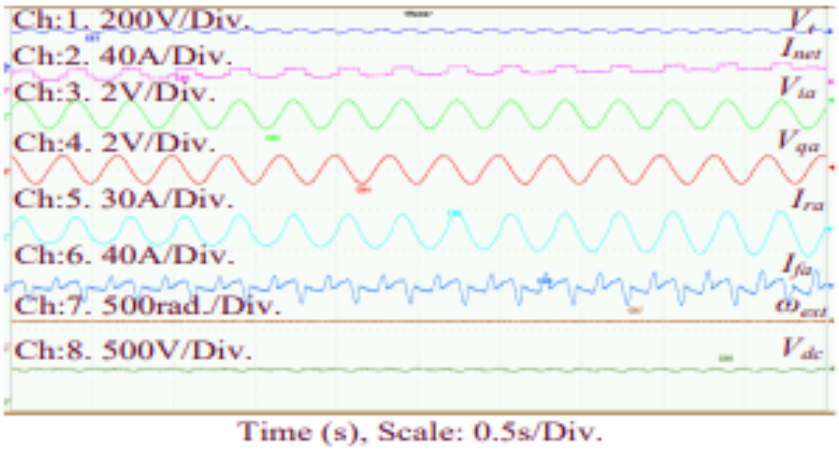

Figure 4.46: Under unbalanced voltage conditions, the control characteristics

Features	IRP	SRF	Fryze	Adaline	Proposed
PLL-needed	NO	YES	NO	NO	NO
Clark's/Park'stransf. needed	YES	YES	NO	NO	NO
Steady-state convergence	$16*10^{-3}$s	$22*10^{-3}$s	$15*10^{-3}$s	$28*10^{-3}$s	$21*10^{-3}$s
THD of grid-current (Isa) %	3.15%	3.58%	3.33%	4.28%	2.162%
FC-extraction	NA	NA	NA	NA	YES
Sampling-time	50 µs	50 µs	50 µs	50 µs	50 µs

Figure 4.47: Proposed Control Algorithms Compared Against Existing Control Schemes

Features	P	PI	PID	FPID
Type-of-controller	Traditional	Traditional	Traditional	Adaptive
Tuning-of-gain parameters	Manual	Manual	Manual	Self-Tuning
Raise time	High	High	High	Low
Settling time	High	High	High	Low
Dynamic performance	Low	Medium	Good	Better
% Of error	High	High	Medium	Very-less
Steady-state behavior	Moderate	Good	Good	Better
Delay time	High	Medium	Moderate	Low

Figure 4.48: A Comparison Of Fuzzy Tuned Pid And Traditional Control Schemes

V. EPILOGUE

In this work, a novel approach (MROGI-FLL) for monitoring the grid-tied PV system's interface inverter to minimize harmonics was examined. We employed a Fuzzy adjusted PID to reduce steady-state error (FPID). Comparing to the old method, in this new circuit topology, voltage level can be maintained and DC-bus connections, the voltage is always the same, by mixing a number of active ingredients that are PWM & PV array, and Control methods, in the external loads. Therefore, We can adjust the DC-DC converter to enhance the PV system's power production. Adaptive evaluation of amplitude, frequency, and phase angle is used in the MROGI-FLL control approach provided here to correct for load and grid harmonics. Detailed discussion is given on the comparison between fuzzy adjusted PID and conventional control methods.

VI. REFERENCES

[1] X. Liang and Ch. Andalib-Bin-Karim, (2018)'Harmonics and Mitigation Techniques Through Advanced Control in Grid-Connected Renewable Energy Sources: A Review', IEEE Transactions on Industry Applications, vol. 54, no. 4, pp. 3100-3111,

[2] P. Acuna, L. MorA¡n, M. Rivera, J. Dixon, and J. Rodriguez, (2014) 'Improved ˜ active power filter performance for renewable power generation systems', IEEE Transactions on Power Electronics, vol. 29, pp. 687-694,

[3] S. K. Khadem, M. Basu, and M. F. Conlon, (2014)'Harmonic power compensation capacity of shunt active power filter and its relationship with design parameters', IET Power Electronics, vol. 7, pp. 418-430,

[4] S. Mikkili, and A. Panda, (2012) 'Real-time implementation of PI and fuzzy logic controllers based shunt active filter control strategies for power quality improvement', International Journal of Electrical Power and Energy Systems, vol. 43, pp. 1114-1126,

[5] A. K. Panda and R. Patel (2015)'Adaptive hysteresis and fuzzy logic controlled based shunt active power filter resistant to shoot-through phenomenon', IET Power Electronics, vol. 8, no. 10, pp. 1963-1977,

[6] P. N. Babu, B. Kar and B. Halder, (2016)'Modelling and analysis of a hybrid active power filter for power quality improvement using hysteresis current control technique', IEEE 7th India International Conference on Power Electronics (IICPE), pp.1-6, 2016.

[7] S. Zeliang, G. Yuhua, and L. Jisan, (2008)'Steady-State and Dynamic Study of Active Power Filter With Efficient FPGA-Based Control Algorithm' IEEE Transactions on Industrial Electronics, vol. 55, no.4, pp.1527- 1536,

[8] P. N. Babu, B. Kar and B. Halder, (2016) 'Comparative analysis of a Hybrid active power filter for power quality improvement using different compensation techniques,' IEEE International Conference on Recent Advances and Innovations in Engineering (ICRAIE), pp.1-6,

[9]M. Qasim, and V. Khadkikar, (2014). 'Application of Artificial Neural Networks for Shunt Active Power Filter Control' IEEE Transactions on Industrial Informatics, vol. 10, no.3, pp. 1765-1774,

[10] J. Kanieski, R. Cardoso, H. Pinheiro et al, (2013). 'Kalman filter-based control system for power quality conditioning devices', IEEE Transactions on Industrial Electronics, vol. 60, no. 11, pp. 5214-5227,

[11] M. A. S. Masoum, S. Jamali, and N. Ghaffarzadeh, (2010).'Detection and classification of power quality disturbances using discrete wavelet transform and wavelet networks', IET Science Measurement & Technology, vol. 4, no. 4, pp. 193-205,

[12] M. A. Platas-Garza and J. A. de la O Serna, (2014). 'Polynomial Implementation of the Taylor-Fourier Transform for Harmonic Analysis', IEEE Transactions on Instrumentation and Measurement, vol. 63, no. 12, pp. 2846-2854,

[13] J. Moriano, M. Rizo, E. J. Bueno, R. Martin and F. J. Rodriguez, (2018).'A Novel Multifrequency Current Reference Calculation to Mitigate Active Power Fluctuations,' IEEE Transactions on Industrial Electronics, vol. 65, no. 1, pp. 810-818,

[14] P. N. Babu, B. C. Babu, P. R. Babu and G. Panda,"(2020). An optimal current control scheme in grid-tied hybrid energy system with active power filter for harmonic mitigation", International Trans. on Elect. and Energy Sys., vol. 30, no.3, e12183, DOI: 10.1002/2050-7038.12183,

[15] S. G. Jorge, C. A. Busada, and J. A. Solsona, (2012).'Frequency adaptive discrete filter for grid synchronization under distorted voltages,' IEEE Transactions on Power Electronics, vol. 27, no. 8, pp. 3584-3594,

[16] S. Golestan, J. M. Guerrero, J. Vasquez, A. M. Abusorrah, and Y. A. Al-Turki, (2019).'A study on three-phase FLLs,' IEEE Transactions on Power Electronics, vol. 34, no. 1, pp.213-224,

[17] E. Guest and N. Mijatovic, (2019).'Discrete-time complex band pass filters for three-phase converter systems', IEEE Transactions on Industrial Electronics, vol. 66, no. 6, pp. 4650-4660,

[18] S. Golestan, J. M. Guerrero and J. C. Vasquez, (2019).'Is Using A Complex Control Gain in Three-phase FLLs Reasonable?', IEEE Transactions on Industrial Electronics, Early Access,

[19] WEIDONG XIAO, 'Photovoltaic Power System: Modeling, Design, and Control'.

[20] Ali M. ELtamaly, ALmoataz Y.ABDELAZIZ, ' Modern Maximum Power Point Tracking Techniques for Photovoltaic Energy Systems.

[21] Adel A.Elbaset / Saad Awad Mohamed Abdelwahab / Hamed anwer Ibrahim / Mohammed Abdelmowgoud Elsayed Eid, 'Performance Analysis of Photovoltaic Systems with Energy Storage Systems'.

[22] Nabil Derbel، Quanmin Zhu, 'Modeling, Identification and Control Methods in Renewable Energy Systems'.

[23] Dimiter Driankov Hans Hellendoorn Michael Reinfrank, 'An Introduction to FUZZY Control'.

[24] P.N. Babu, P.R Babu and G. Panda, (2019). 'An Adaptive Differentiation Frequency based Advanced Reference current Generator in Grid-tied PV Applications', IEEE Journal of Emerging and Selected Topics in Power Electronics, Early Access, Aug-2019.

[25] I. Sefa, N. Altin, S.Ozdemir, and O.Kaplan, (2015).' Fuzzy PI controlled inverter for grid interactive renewable energy system', IET Rene. Power Gene., vol.9, no.7, pp. 729-738,

RESUME

Name Surname: Mousa Mohammed

Education:

High School completed from Al-Wataneya School (Hawalli) : June 2015

90.41%

2015-2019 Bachelor's degree in Biomedical Engineering from Kharkiv National University of Radio Electronic.

2012-2018 İstanbul Aydın University-Master's, Electrical and Electronics Engineering.

Work Experience:

Work as trainee in ATC (Advanced Technology Company) for 12 months.

Languages:

-Arabic: Native Language

-English: Advanced

Skills:

-Communication, Teamwork, Problem Solving, Flexibility, Creativity

- Computer skills (Microsoft Office) and others

- Good in use Matlab Simulink.

- Good in use (Multisim, Mathcad, AutoCAD, and MATLAB).